



Numerical solution of some stiff systems arising in chemistry via Taylor wavelet collocation method

G. Manohara¹ · S. Kumbinarasaiah¹

Received: 12 June 2023 / Accepted: 8 August 2023 / Published online: 18 September 2023
© The Author(s), under exclusive licence to Springer Nature Switzerland AG 2023

Abstract

This paper presents the innovative Taylor wavelet collocation method (TWCM) for the stiff systems arising in chemical reactions. In this technique, first, we generated the functional matrix of integration (FMI) for the Taylor wavelets. Using this FMI, the Taylor wavelet collocation method is proposed to obtain the numerical approximation of stiff systems in the form of a system of ordinary differential equations (SODEs). This method converts the SODEs into a set of algebraic equations, which can be solved by the Newton–Raphson method. To demonstrate the simplicity and effectiveness of the presented approach, numerical results are obtained. Graphs and tables illustrate the created strategy’s effectiveness and consistency. Illustrative examples are examined to demonstrate the performance and effectiveness of the developed approximation technique, and a comparison is made with the current results. Results reveal that the newly selected strategy is superior to previous approaches regarding precision and effectiveness in the literature. Most semi-analytical and numerical methods work based on controlling parameters, but this technique is free from controlling parameters. Also, it is easy to implement and consumes less time to handle the system. The suggested wavelet-based numerical method is computationally appealing, successful, trustworthy, and resilient. All computations have been made using the Mathematica 11.3 software. The convergence of this strategy is explained using theorems.

Keywords Taylor wavelet · System of ordinary differential equations · Collocation technique · Stiff systems · Chemical problems

Mathematics Subject Classification 34B16 · 34A12 · 6L05 · 65L10

✉ S. Kumbinarasaiah
kumbinarasaiah@gmail.com

G. Manohara
manoharavdc15@gmail.com

¹ Department of Mathematics, Bangalore University, Bengaluru 560 056, India

1 Introduction

Stiff systems of ordinary differential equations are a significant special case of the systems taken up in Initial Value Problems. There is no universally accepted definition of stiffness. Some attempts to understand stiffness examine the behaviour of fixed step size solutions of linear ordinary differential equations systems with constant coefficients [1]. Nonlinear ordinary stiff differential equations are generated by various physical systems, including nuclear reactors, laser oscillators, and others, and their magnitude of eigenvalues can fluctuate significantly. Additionally, the solutions to some differential equations can vary on different time scales, distinguishing them from other equations. These differential equations are often referred to as stiff. It is common for stiff problems to occur in fields like chemical kinetics, climatology, fluid dynamics, ionospheric physics, biochemistry, control theory, electronics, etc., when the equilibrium solution slowly changes while the transients rapidly decrease. Stability and accuracy are the two major issues associated with stiff systems. In some circumstances, the traditional single-step approaches are ineffective because a small step size can result in adequate round-off error to create instability. Despite equations may take longer time to compute. The essence of the difficulty is that when solving non-stiff problems, a step size small enough to provide the desired accuracy is small enough that the stability of the numerical method is qualitatively the same as that of the differential equations. For a stiff problem, step sizes that would provide an accurate solution with an explicit Runge–Kutta method must be reduced significantly to keep the computation stable. An equally important practical matter is that strategies with superior stability properties cannot be evaluated by simple iteration for non-stiff problems because the step size must be very small for the iteration to converge. In practice, stiffness of an initial value problem is depends on the stability of the problem, the length of the interval of integration, the stability of the numerical method, and how the method is implemented. Often the best way to proceed is to try one of the solvers intended for non-stiff systems. If it is unsatisfactory, the problem may be stiff [1].

Consider the general form of the system of stiff ODEs:

$$\left. \begin{aligned} y'(\xi) &= F(y(\xi), z(\xi), \xi) \\ z'(\xi) &= G(y(\xi), z(\xi), \xi) \end{aligned} \right\} \quad (1.1)$$

where y and z are dependent variables, and ξ is an independent variable with primary constraints: $y(0) = \alpha$ and $z(0) = \beta$, where $\alpha, \beta \in \mathbb{R}$. A significant amount of research has been done on Stiff systems arising in the chemical field, including a solution to the stiff system of IVPs that converge quickly provided by Carrol [2]. Hojjati et al. insisted adaptive method called EMBDF for the numerical solution of stiff systems [3], Cash JR implemented an extended backward differentiation formula for the stiff problems [4], Hosseini proposed matrix-free MEBDF method for the solution of stiff systems of ODEs [5], Hsiao insisted Haar wavelet approach to stiff linear systems [6], Bujurke NM proposed the numerical solution of stiff systems using single term Haar wavelet series [7]. In [8], Darvishi MT et al. illustrated the variational iteration method for the linear and nonlinear stiff problems. Badar

G et al. implemented a semi-implicit mid-point rule for stiff systems [9], and Prothero A proposed the stability and accuracy of the one-step method for solving stiff systems [10]. But neither the computation effort nor the stability requirement has been significantly reduced by these methods. Here, we imposed the wavelet-based numerical method called the Taylor wavelet collocation scheme to overcome issues like the stability and accuracy of the systems.

Wavelets are built on Joseph Fourier's fundamental theory of superpositioning, which states that a collection of self-similar functions can express a complex function. With the help of wavelets, which are mathematical processes, data may be divided into different frequency components, and each component can then be analyzed with a resolution that matches its scale. Wavelet theory has recently attracted much interest because of its numerous valuable applications in system analysis, numerical analysis, and optimal control. A wavelet is an oscillation resembling a wave with an amplitude that begins at zero, increases or decreases, and then repeats one or more times. Wavelets have several characteristics that support their application in numerically solving differential equations. The orthogonal, compactly supported wavelet basis precisely approximates an increasingly higher-order polynomial. This wavelet-based representation of differential operations can be precise and stable even in areas with significant gradients or oscillations. Numerous dynamical system problems have extensively used approximate solutions using an orthogonal family of functions. Using truncated orthogonal functions to approximate the various signals in the equation, one can approximate the underlying differential equation using orthogonal functions. The functional integration matrix can then be used to eliminate the integral operations. Although the Taylor series and Fibonacci polynomials are not built on orthogonal functions, they have the operational integration matrix. Orthogonal wavelet basis also has the advantage of multi-resolution analysis over conventional techniques. For some of the common mathematical problems, various wavelet collocation techniques have been used, such as the Chebyshev wavelet collocation method [11], collocation method based on Bernoulli and Gegenbauer wavelets [12], Hermite wavelet collocation method [13, 14], Laguerre wavelet collocation method [15]. Several wavelet collocation techniques are typically employed to solve fractional differential equations, which include Haar wavelets [16], Chelyshkov wavelets [17], Fibonacci wavelets [18], Cubic B Spline [19], Chebyshev wavelets [20], Genocchi wavelets [21], Bernoulli wavelets [22–24], Legendre wavelet tau method [25], Hermite wavelets [26, 27], Legendre wavelets and Gegenbauer wavelets [28].

The current work's objective is to create a Taylor wavelets collocation method that is fast and simple. A recent addition to the wavelet families is the Taylor wavelets formed by Taylor polynomials. It guarantees the required accuracy for relatively small grid points to solve stiff systems. It is challenging to find the necessary approximations using a new numerical design.

The significance of the proposed method (TWCM) is as follows:

- The number of terms of the Taylor polynomials $T_m(x)$ is less than the number of the terms of the other polynomials, say Bernoulli polynomials $B_m(x)$, Fibonacci

polynomials $F_m(x)$, and Legendre polynomials $L_m(x)$. It helps to reduce the CPU time.

- Error components in the FMI representing Taylor polynomials are less than that of other polynomials.
- Taylor polynomials have less coefficient of individual terms than corresponding ones in other polynomials. Computational errors can be reduced using this property.
- Taylor wavelets are superior wavelets not based on orthogonal polynomials, but we can express the Taylor polynomials in approximating orthogonal polynomials.
- The Taylor wavelet method is suitable for solutions with sharp edge/ jump discontinuities.
- Fractional differential equations, delay differential equations, and stiff systems can be solved using this method directly without using any control parameters.
- The Taylor wavelet method can solve the higher-order system of ordinary differential equations by slightly modifying the method.
- This method can be extended to PDEs and other mathematical models with different physical conditions.
- It is used to obtain the solution of the differential equation in the universal domain by taking the suitable transformation.

Wavelet approaches for resolving differential and integral equations have recently received greater attention. Researchers start using this package to solve mathematical problems such as Bratu- type equations [29], fractional delay differential equations [30], systems of nonlinear fractional differential equations with application to human respiratory syncytial virus infection [31], Benjamin-Bona-Mohany PDEs [32], Burger's equation [33], Biological models [34], linear and nonlinear Lane-Emden equations [35], Chemistry problems [36], reaction-diffusion problems in science and engineering [37, 38], Fisher's equations [39], and nonlinear Parabolic equations [40]. Here, the Taylor wavelet collocation technique was successfully applied to the system, and significant approximation was obtained in the system's solution. To our knowledge, no one solved these stiff systems by Taylor wavelets which motivates us to study this by the developed strategy. The absolute error with the Exact solution and ND Solver solution for numerous values of M and k are computed to validate the efficacy and precision of the developed strategy.

This article's structure is as follows: Sect. 2, named "Preliminaries" provides the definitions of wavelets. FMI of Taylor wavelets carried out in Sect. 3. The method of solution and application of the newly developed strategy is described in Sect. 4 and Sect. 5, respectively. Finally, Sect. 6 provides the conclusion of the article.

2 Preliminaries of Taylor wavelets and some theorems

2.1 Taylor wavelets

On the interval $[0, 1]$, the Taylor wavelets are defined as [29],

$$\mathfrak{S}_{n,m}(\xi) = \begin{cases} 2^{\frac{k-1}{2}} T_m(2^{k-1}\xi - n + 1), & \frac{n-1}{2^{k-1}} \leq \xi < \frac{n}{2^{k-1}} \\ 0, & \text{Otherwise} \end{cases}$$

where

$$T_m(\xi) = \sqrt{2m+1} \xi^m,$$

where $T_m(\xi)$ is the normal Taylor polynomial of degree- m , translation parameter $n = 1, 2, \dots, 2^{k-1}$ and, k represents the level of resolution $k = 1, 2, \dots$ and respectively. The quantity $\sqrt{2m+1}$ is a normalization factor. Taylor wavelets are compactly supported wavelets formed by Taylor polynomials over the interval $[0, 1]$.

Theorem 1. Let H be a Hilbert space and W be a closed subspace of H such that $\dim W < \infty$ and $\{w_1, w_2, \dots, w_n\}$ is any basis for W . Let g be an arbitrary element in H and g_0 be the unique best approximation to g out of W . Then. [29]

$\|g - g_0\|_2 = G_g$, Where $G_g = \left(\frac{Z(g, w_1, w_2, \dots, w_n)}{Z(g, w_1, w_2, \dots, w_n)} \right)^{\frac{1}{2}}$ and Z is introduced [29] as follows:

$$Z(g, w_1, w_2, \dots, w_n) = \begin{vmatrix} \langle g, g \rangle & \langle g, w_1 \rangle & \dots & \langle g, w_n \rangle \\ \langle w_1, g \rangle & \langle w_1, w_1 \rangle & \dots & \langle w_1, w_n \rangle \\ \dots & \dots & \dots & \dots \\ \langle w_n, g \rangle & \langle w_n, w_1 \rangle & \dots & \langle w_n, w_n \rangle \end{vmatrix}$$

Theorem 2: Let $L^2[0, 1]$ be the Hilbert space generated by the Taylor wavelet basis. Let $\eta(\xi)$ be the continuous bounded function in $L^2[0, 1]$. Then the Taylor wavelet expansion of $\eta(\xi)$ converges with it.

Proof: Let $\eta : [0, 1] \rightarrow R$ be a continuous function and $|\eta(\xi)| \leq \mu$, where μ be any real number. Then Taylor wavelet dilation of $y(\xi)$ can be expressed as,

$$\begin{aligned} \eta(\xi) &= \sum_{n=1}^{2^{\frac{k-1}{2}}} \sum_{m=0}^{M-1} a_{n,m} \mathfrak{S}_{n,m}(\xi). \\ a_{n,m} &= \langle \eta(\xi), \mathfrak{S}_{n,m}(\xi) \rangle \text{ Denotes inner product.} \\ a_{n,m} &= \int_0^1 \eta(\xi) \mathfrak{S}_{n,m}(\xi) d\xi, \end{aligned}$$

Since $\mathfrak{S}_{n,m}$ are the orthogonal basis.

$$a_{n,m} = \int_I \eta(\xi) T_m(2^{k-1}\xi - n + 1) d\xi \text{ where } I = \left[\frac{n-1}{2^{k-1}}, \frac{n}{2^{k-1}} \right)$$

Since $T_m(\xi) = \sqrt{2m+1} \xi^m$, we obtain.

$$a_{n,m} = \int_I \eta(\xi) \sqrt{2m+1} (2^{k-1}\xi - n + 1)^m d\xi \text{ where } I = \left[\frac{n-1}{2^{k-1}}, \frac{n}{2^{k-1}} \right)$$

Then substitute $2^{k-1}\xi - n + 1 = y$ then we get,

$$a_{n,m} = \frac{2^{\frac{k-1}{2}}}{\sqrt{2m+1}} \int_0^1 \eta\left(\frac{y+n-1}{2^{k-1}}\right) y^m \frac{dy}{2^{k-1}}$$

$$a_{n,m} = \frac{2^{\frac{1-k}{2}}}{\sqrt{2m+1}} \int_0^1 \eta\left(\frac{y+n-1}{2^{k-1}}\right) y^m dy$$

By generalized mean value theorem,

$$a_{n,m} = \frac{2^{\frac{-k+1}{2}}}{\sqrt{2m+1}} \eta\left(\frac{\delta+n-1}{2^{k-1}}\right) \int_0^1 y^m dy \text{ for some } \delta \in (0, 1)$$

Since y^m is a bounded continuous function. Put $\int_0^1 y^m dy = h$

$$|a_{n,m}| = \left| \frac{2^{\frac{-k+1}{2}}}{\sqrt{2m+1}} \right| \left| \eta\left(\frac{\delta+n-1}{2^{k-1}}\right) \right| h$$

Since η remains bounded.

$$\text{Hence, } |a_{n,m}| = \left| \frac{2^{\frac{-k+1}{2}}}{\sqrt{2m+1}} \mu h \right| \text{ where } \mu = \eta\left(\frac{\delta+n-1}{2^{k-1}}\right)$$

Therefore, $\sum_{n,m=0}^{\infty} a_{n,m}$ is absolutely convergent. Hence the Taylor wavelet series expansion $\eta(\xi)$ converges uniformly to it.

Remarks: Error estimation for continuous bounded function $\eta(\xi)$ by using the above theorem 2.

$\eta(\xi)$ is the exact solution and $\eta_{app}(\xi)$ is the Taylor wavelet approximation.

$$\text{Where, } \eta(\xi) = \sum_{n=1}^{\infty} \sum_{m=0}^{\infty} a_{n,m} S_{n,m}(\xi) \text{ and } \eta_{app}(\xi) = \sum_{n=1}^{2^{\frac{k-1}{2}}} \sum_{m=0}^{M-1} a_{n,m} S_{n,m}(\xi).$$

$$\eta(\xi) - \eta_{app}(\xi) = \sum_{n=1}^{\infty} \sum_{m=0}^{\infty} a_{n,m} S_{n,m}(\xi) - \sum_{n=1}^{2^{\frac{k-1}{2}}} \sum_{m=0}^{M-1} a_{n,m} S_{n,m}(\xi) = \sum_{n=2^k}^{\infty} \sum_{m=M}^{\infty} a_{n,m} S_{n,m}(\xi)$$

$$\text{Now, } \|E_n\|^2 = \|\eta(\xi) - \eta_{app}(\xi)\|^2 = \langle \eta(\xi) - \eta_{app}(\xi), \eta(\xi) - \eta_{app}(\xi) \rangle$$

$$\Rightarrow \|E_n\|^2 = \int_0^1 \sum_{n=2^k}^{\infty} \sum_{m=M}^{\infty} a_{n,m}^2 S_{n,m}^2(\xi)$$

$$\text{But from the above theorem, we have, } |a_{n,m}| \leq \left| \frac{2^{\frac{-k+1}{2}}}{\sqrt{2m+1}} \mu h \right|$$

$$\Rightarrow \|E_n\|^2 \leq \int_0^1 \sum_{n=2^k}^{\infty} \sum_{m=M}^{\infty} \frac{2^{-k+1}}{2m+1} \mu^2 h^2 S_{n,m}^2(\xi).$$

Theorem 3 [41]: *Let the Taylor wavelet sequence $\{\lambda_{n,m}^k(\xi)\}_{k=1}^{\infty}$ which are continuous functions defined in $L^2(\mathbb{R})$ in ξ on $[a, b]$ converges to the function $\mathcal{S}(\xi)$ in $L^2(\mathbb{R})$ uniformly in ξ on $[a, b]$. Then $\mathcal{S}(\xi)$ is continuous in $L^2(\mathbb{R})$ in ξ on $[a, b]$.*

Theorem 4 [41]: Let the Taylor wavelet sequence $\{\lambda_{n,m}^k(\xi)\}_{k=1}^{\infty}$ converges itself in $L_2(\mathbb{R})$ uniformly in ξ on $[a, b]$. Then there is a function $\mathfrak{S}(\xi)$ is continuous in $L_2(\mathbb{R})$ in ξ on $[a, b]$ and $\lim_{k \rightarrow \infty} \lambda_{n,m}^k(\xi) = \lambda_{n,m}(\xi) \forall t \in [a, b]$.

Theorem 2 [23]: Let $I \subset \mathbb{R}$ be a finite interval with length $m(I)$. Furthermore, $f(\xi)$ is an integrable function defined on I and $\sum_{i=0}^{M-1} \sum_{j=1}^{2^{k-1}} a_{i,j} \mathfrak{S}_{i,j}(\xi)$ be a good Taylor wavelet approximation of f on I with for some $\epsilon > 0$, $|f(\xi) - \sum_{i=0}^{M-1} \sum_{j=1}^{2^{k-1}} a_{i,j} \mathfrak{S}_{i,j}(\xi)| \leq \epsilon, \forall x \in I$. Then $-\epsilon m(I) + \int_I \sum \sum a_{i,j} \mathfrak{S}_{i,j}(\xi) d\xi \leq \int_I f(\xi) d\xi \leq \epsilon m(I) + \int_I \sum \sum a_{i,j} \mathfrak{S}_{i,j}(\xi) d\xi$.

This theorem says that when an integral of a complicated function is impossible, it can be evaluated by approximately the $f(\xi)$ by wavelet functions in a given interval.

3 Functional matrix of integration (FMI)

At $k = 1$ and $M = 6$, the Taylor wavelet basis is obtained as below:

$$\mathfrak{S}_{1,0}(\xi) = 1$$

$$\mathfrak{S}_{1,1}(\xi) = \sqrt{3}\xi$$

$$\mathfrak{S}_{1,2}(\xi) = \sqrt{5}\xi^2$$

$$\mathfrak{S}_{1,3}(\xi) = \sqrt{7}\xi^3$$

$$\mathfrak{S}_{1,4}(\xi) = 3\xi^4$$

$$\mathfrak{S}_{1,5}(\xi) = \sqrt{11}\xi^5$$

$$\mathfrak{S}_{1,6}(\xi) = \sqrt{13}\xi^6$$

$$\mathfrak{S}_{1,7}(\xi) = \sqrt{15}\xi^7$$

Integrating the above first six basis regarding ξ limit from 0 to ξ , and the Taylor wavelet bases are then stated as a linear combination as;

$$\int_0^{\xi} \mathfrak{S}_{1,0}(\xi) d\xi = \begin{bmatrix} 0 & \frac{1}{\sqrt{3}} & 0 & 0 & 0 & 0 \end{bmatrix} \mathfrak{S}_6(\xi)$$

$$\int_0^\xi \mathfrak{S}_{1,1}(\xi) d\xi = \begin{bmatrix} 0 & 0 & \frac{\sqrt{\frac{3}{5}}}{2} & 0 & 0 & 0 \end{bmatrix} \mathfrak{S}_6(\xi)$$

$$\int_0^\xi \mathfrak{S}_{1,2}(\xi) d\xi = \begin{bmatrix} 0 & 0 & 0 & \frac{\sqrt{\frac{5}{7}}}{3} & 0 & 0 \end{bmatrix} \mathfrak{S}_6(\xi)$$

$$\int_0^\xi \mathfrak{S}_{1,3}(\xi) d\xi = \begin{bmatrix} 0 & 0 & 0 & 0 & \frac{\sqrt{7}}{12} & 0 \end{bmatrix} \mathfrak{S}_6(\xi)$$

$$\int_0^\xi \mathfrak{S}_{1,4}(\xi) d\xi = \begin{bmatrix} 0 & 0 & 0 & 0 & 0 & \frac{3}{5\sqrt{11}} \end{bmatrix} \mathfrak{S}_6(\xi)$$

$$\int_0^\xi \mathfrak{S}_{1,5}(\xi) d\xi = \begin{bmatrix} 0 & 0 & 0 & 0 & 0 & 0 \end{bmatrix} \mathfrak{S}_6(\xi)$$

$$\int_0^\xi \mathfrak{S}(\xi) d\xi = \mathbb{B}_{6 \times 6} \mathfrak{S}_6(\xi) + \bar{\mathfrak{S}}_6(\xi) \quad (3.1)$$

where,

$$\mathfrak{S}_6(\xi) = [\mathfrak{S}_{1,0}(\xi), \mathfrak{S}_{1,1}(\xi), \mathfrak{S}_{1,2}(\xi), \mathfrak{S}_{1,3}(\xi), \mathfrak{S}_{1,4}(\xi), \mathfrak{S}_{1,5}(\xi)]^T$$

$$\mathbb{B}_{6 \times 6} = \begin{bmatrix} 0 & \frac{1}{\sqrt{3}} & 0 & 0 & 0 & 0 \\ 0 & 0 & \frac{\sqrt{\frac{3}{5}}}{2} & 0 & 0 & 0 \\ 0 & 0 & 0 & \frac{\sqrt{\frac{5}{7}}}{3} & 0 & 0 \\ 0 & 0 & 0 & 0 & \frac{\sqrt{7}}{12} & 0 \\ 0 & 0 & 0 & 0 & 0 & \frac{3}{5\sqrt{11}} \\ 0 & 0 & 0 & 0 & 0 & 0 \end{bmatrix}, \bar{\mathfrak{S}}_6(\xi) = \begin{bmatrix} 0 \\ 0 \\ 0 \\ 0 \\ 0 \\ \frac{\sqrt{\frac{11}{13}}}{6} \mathfrak{S}_{1,6}(\xi) \end{bmatrix}$$

The generalized functional matrix of integration of n -wavelet basis at $k = 1$ is defined as:

$$\int_0^\xi \mathfrak{S}(\xi)d\xi = \mathbb{B}_{n \times n} \mathfrak{S}(\xi) + \bar{\mathfrak{S}}_n(\xi),$$

where,

$$\mathbb{B}_{n \times n} = \begin{bmatrix} 0 & \frac{1}{\sqrt{3}} & 0 & 0 & 0 & \dots & 0 & 0 \\ 0 & 0 & \frac{\sqrt{3}}{2\sqrt{5}} & 0 & 0 & \dots & 0 & 0 \\ 0 & 0 & 0 & \frac{\sqrt{5}}{3\sqrt{7}} & 0 & \dots & 0 & 0 \\ 0 & 0 & 0 & 0 & \frac{\sqrt{7}}{12} & \dots & 0 & 0 \\ \vdots & \vdots & \vdots & \vdots & \ddots & \ddots & 0 & 0 \\ 0 & 0 & 0 & 0 & 0 & 0 & \frac{\sqrt{2(n-2)+1}}{(n-1)\sqrt{2(n-2)+3}} & 0 \\ 0 & 0 & 0 & 0 & 0 & \dots & 0 & \frac{\sqrt{2(n-1)+1}}{n\sqrt{2(n-1)+3}} \\ 0 & 0 & 0 & 0 & 0 & \dots & 0 & 0 \end{bmatrix}$$

and

$$\bar{\mathfrak{S}}_n(\xi) = \begin{bmatrix} 0 \\ 0 \\ 0 \\ 0 \\ 0 \\ 0 \\ \vdots \\ \frac{\sqrt{2n-1}}{n\sqrt{2n+1}} \mathfrak{S}_{1,n}(\xi) \end{bmatrix}.$$

Integrating the basis stated above again, we attain the following;

$$\int_0^\xi \int_0^\xi \mathfrak{S}_{1,0}(\xi)d\xi = \left[0 \ 0 \ \frac{1}{2\sqrt{5}} \ 0 \ 0 \ 0 \right] \mathfrak{S}_6(\xi)$$

$$\int_0^\xi \int_0^\xi \mathfrak{S}_{1,1}(\xi)d\xi = \left[0 \ 0 \ 0 \ \frac{1}{2\sqrt{21}} \ 0 \ 0 \right] \mathfrak{S}_6(\xi)$$

$$\int_0^\xi \int_0^\xi \mathfrak{S}_{1,2}(\xi)d\xi = \left[0 \ 0 \ 0 \ 0 \ \frac{\sqrt{5}}{36} \ 0 \right] \mathfrak{S}_6(\xi)$$

$$\int_0^\xi \int_0^\xi \mathfrak{S}_{1,3}(\xi)d\xi = \left[0 \ 0 \ 0 \ 0 \ 0 \ \frac{\sqrt{\frac{7}{11}}}{20} \right] \mathfrak{S}_6(\xi)$$

$$\int_0^\xi \int_0^\xi \mathfrak{S}_{1,4}(\xi) d\xi = [0 \ 0 \ 0 \ 0 \ 0 \ 0] \mathfrak{S}_6(\xi)$$

$$\int_0^\xi \int_0^\xi \mathfrak{S}_{1,5}(\xi) d\xi = [0 \ 0 \ 0 \ 0 \ 0 \ 0] \mathfrak{S}_6(\xi)$$

Hence,

$$\int_0^\xi \int_0^\xi \mathfrak{S}(\xi) d\xi = \mathbb{B}'_{6 \times 6} \mathfrak{S}_6(\xi) + \bar{\mathfrak{S}}'_6(\xi) \tag{3.2}$$

where $\mathbb{B}'_{6 \times 6} = \begin{bmatrix} 0 & 0 & \frac{1}{2\sqrt{5}} & 0 & 0 & 0 \\ 0 & 0 & 0 & \frac{1}{2\sqrt{21}} & 0 & 0 \\ 0 & 0 & 0 & 0 & \frac{\sqrt{5}}{36} & 0 \\ 0 & 0 & 0 & 0 & 0 & \frac{\sqrt{\frac{7}{11}}}{20} \\ 0 & 0 & 0 & 0 & 0 & 0 \\ 0 & 0 & 0 & 0 & 0 & 0 \end{bmatrix}, \bar{\mathfrak{S}}'_6(\xi) = \begin{bmatrix} 0 \\ 0 \\ 0 \\ 0 \\ \frac{1}{10\sqrt{13}} \mathfrak{S}_{1,6}(\xi) \\ \frac{\sqrt{\frac{11}{15}}}{42} \mathfrak{S}_{1,7}(\xi) \end{bmatrix}$

The Taylor wavelet basis is examined at $k = 2$ and $M = 6$ as follows:

$$\left. \begin{aligned} \mathfrak{S}_{1,0}(\xi) &= \sqrt{2} \\ \mathfrak{S}_{1,1}(\xi) &= 2\sqrt{6}\xi \\ \mathfrak{S}_{1,2}(\xi) &= 4\sqrt{10}\xi^2 \\ \mathfrak{S}_{1,3}(\xi) &= 8\sqrt{14}\xi^3 \\ \mathfrak{S}_{1,4}(\xi) &= 48\sqrt{2}\xi^4 \\ \mathfrak{S}_{1,5}(\xi) &= 32\sqrt{22}\xi^5 \end{aligned} \right\} 0 \leq \xi < \frac{1}{2}$$

$$\left. \begin{aligned} \mathfrak{S}_{2,0}(\xi) &= \sqrt{2} \\ \mathfrak{S}_{2,1}(\xi) &= \sqrt{6}(-1 + 2\xi) \\ \mathfrak{S}_{2,2}(\xi) &= \sqrt{10}(1 - 2\xi)^2 \\ \mathfrak{S}_{2,3}(\xi) &= \sqrt{14}(-1 + 2\xi)^3 \\ \mathfrak{S}_{2,4}(\xi) &= 3\sqrt{2}(1 - 2\xi)^4 \\ \mathfrak{S}_{2,5}(\xi) &= \sqrt{22}(-1 + 2\xi)^5 \end{aligned} \right\} \frac{1}{2} \leq \xi < 1$$

$$\int_0^\xi \mathfrak{S}(\xi) d\xi = \mathbb{B}_{12 \times 12} \mathfrak{S}_{12}(\xi) + \bar{\mathfrak{S}}_{12}(\xi) \tag{3.3}$$

where $S_{12}(\xi) = [S_{1,0}(\xi), S_{1,1}(\xi), S_{1,2}(\xi), S_{1,3}(\xi), S_{1,4}(\xi), S_{1,5}(\xi), S_{2,0}(\xi), S_{2,1}(\xi), S_{2,2}(\xi), S_{2,3}(\xi), S_{2,4}(\xi), S_{2,5}(\xi)]^T$

$$\mathbb{R}_{12 \times 12} = \begin{bmatrix} 0 & \frac{1}{2\sqrt{3}} & 0 & 0 & 0 & 0 & 0 & 0 & 0 & 0 & 0 & 0 \\ 0 & 0 & \frac{\sqrt{3}}{4} & 0 & 0 & 0 & 0 & 0 & 0 & 0 & 0 & 0 \\ 0 & 0 & 0 & \frac{\sqrt{5}}{6} & 0 & 0 & 0 & 0 & 0 & 0 & 0 & 0 \\ 0 & 0 & 0 & 0 & \frac{\sqrt{7}}{24} & 0 & 0 & 0 & 0 & 0 & 0 & 0 \\ 0 & 0 & 0 & 0 & 0 & \frac{3}{10\sqrt{11}} & 0 & 0 & 0 & 0 & 0 & 0 \\ 0 & 0 & 0 & 0 & 0 & 0 & 0 & 0 & 0 & 0 & 0 & 0 \\ 0 & 0 & 0 & 0 & 0 & 0 & 0 & \frac{1}{2\sqrt{3}} & 0 & 0 & 0 & 0 \\ 0 & 0 & 0 & 0 & 0 & 0 & 0 & 0 & \frac{\sqrt{3}}{4} & 0 & 0 & 0 \\ 0 & 0 & 0 & 0 & 0 & 0 & 0 & 0 & 0 & \frac{\sqrt{5}}{6} & 0 & 0 \\ 0 & 0 & 0 & 0 & 0 & 0 & 0 & 0 & 0 & 0 & \frac{\sqrt{7}}{24} & 0 \\ 0 & 0 & 0 & 0 & 0 & 0 & 0 & 0 & 0 & 0 & 0 & \frac{3}{10\sqrt{11}} \\ 0 & 0 & 0 & 0 & 0 & 0 & 0 & 0 & 0 & 0 & 0 & 0 \end{bmatrix},$$

and

$$\bar{S}_{12}(\xi) = \begin{bmatrix} 0 \\ 0 \\ 0 \\ 0 \\ 0 \\ \frac{\sqrt{11}}{12} S_{1,6}(\xi) \\ 0 \\ 0 \\ 0 \\ 0 \\ 0 \\ \frac{\sqrt{11}}{12} S_{2,6}(\xi) \end{bmatrix}$$

The generalized first integration of n -wavelet basis at $k = 2$ is defined as:

$$\int_0^\xi \mathfrak{S}(\xi) d\xi = \mathbb{B}_{2n \times 2n} \mathfrak{S}(\xi) + \bar{\mathfrak{S}}_{2n}(\xi),$$

where

$\mathbb{B}_{2n \times 2n} =$

$$\begin{bmatrix} 0 & \frac{1}{2\sqrt{3}} & 0 & 0 & 0 & \dots & 0 & 0 & 0 & 0 & 0 & 0 & 0 & 0 & 0 & 0 & 0 & 0 & 0 & 0 & 0 \\ 0 & 0 & \frac{\sqrt{\frac{3}{5}}}{4} & 0 & 0 & \dots & 0 & 0 & 0 & 0 & 0 & 0 & 0 & 0 & 0 & 0 & 0 & 0 & 0 & 0 & 0 \\ 0 & 0 & 0 & \frac{\sqrt{\frac{5}{7}}}{6} & 0 & \dots & 0 & 0 & 0 & 0 & 0 & 0 & 0 & 0 & 0 & 0 & 0 & 0 & 0 & 0 & 0 \\ 0 & 0 & 0 & 0 & \frac{\sqrt{7}}{24} & \dots & 0 & 0 & 0 & 0 & 0 & 0 & 0 & 0 & 0 & 0 & 0 & 0 & 0 & 0 & 0 \\ \vdots & \vdots & \vdots & \vdots & \ddots & \ddots & 0 & 0 & 0 & 0 & 0 & 0 & 0 & 0 & 0 & 0 & 0 & 0 & 0 & 0 & 0 \\ 0 & 0 & 0 & 0 & 0 & 0 & \frac{\sqrt{2(n-2)+1}}{(2n-1)\sqrt{2(n-2)+3}} & 0 & 0 & 0 & 0 & 0 & 0 & 0 & 0 & 0 & 0 & 0 & 0 & 0 & 0 \\ 0 & 0 & 0 & 0 & 0 & 0 & 0 & \frac{\sqrt{2(n-1)+1}}{2n\sqrt{2(n-1)+3}} & 0 & 0 & 0 & 0 & 0 & 0 & 0 & 0 & 0 & 0 & 0 & 0 & 0 \\ 0 & 0 \\ 0 & 0 & 0 & 0 & 0 & 0 & 0 & 0 & 0 & \frac{1}{2\sqrt{3}} & 0 & 0 & 0 & \dots & 0 & 0 & 0 & 0 & 0 & 0 \\ 0 & 0 & 0 & 0 & 0 & 0 & 0 & 0 & 0 & 0 & \frac{\sqrt{\frac{3}{5}}}{4} & 0 & 0 & \dots & 0 & 0 & 0 & 0 & 0 & 0 \\ 0 & 0 & 0 & 0 & 0 & 0 & 0 & 0 & 0 & 0 & 0 & \frac{\sqrt{\frac{5}{7}}}{6} & 0 & \dots & 0 & 0 & 0 & 0 & 0 & 0 \\ 0 & 0 & 0 & 0 & 0 & 0 & 0 & 0 & 0 & 0 & 0 & 0 & \frac{\sqrt{7}}{24} & \dots & 0 & 0 & 0 & 0 & 0 & 0 \\ 0 & 0 & 0 & 0 & 0 & 0 & 0 & 0 & \vdots & \vdots & \vdots & \vdots & \ddots & \ddots & \frac{\sqrt{2(n-2)+1}}{(2n-1)\sqrt{2(n-2)+3}} & 0 & 0 & 0 & 0 & 0 \\ 0 & 0 & 0 & 0 & 0 & 0 & 0 & 0 & 0 & 0 & 0 & 0 & 0 & 0 & 0 & 0 & \frac{\sqrt{2(n-1)+1}}{2n\sqrt{2(n-1)+3}} & 0 & 0 & 0 \\ 0 & 0 \end{bmatrix}$$

$$\bar{\mathfrak{S}}_{2n}(\xi) = \begin{bmatrix} 0 \\ 0 \\ 0 \\ 0 \\ 0 \\ \vdots \\ \frac{\sqrt{2n-1}}{2n\sqrt{2n+1}} \mathfrak{S}_{1,n}(\xi) \\ 0 \\ 0 \\ 0 \\ 0 \\ 0 \\ \vdots \\ \frac{\sqrt{2n-1}}{2n\sqrt{2n+1}} \mathfrak{S}_{2,n}(\xi) \end{bmatrix}$$

Similarly, the second integration can be written as:

$$\int_0^\xi \int_0^\xi \mathfrak{S}(\xi) d\xi d\xi = \mathbb{H}'_{12 \times 12} \mathfrak{S}_{12}(\xi) + k \bar{\mathfrak{S}}'_{12}(\xi) \tag{3.4}$$

where $\mathfrak{S}_{12}(\xi) = [\mathfrak{S}_{1,0}(\xi), \mathfrak{S}_{1,1}(\xi), \mathfrak{S}_{1,2}(\xi), \mathfrak{S}_{1,3}(\xi), \mathfrak{S}_{1,4}(\xi), \mathfrak{S}_{1,5}(\xi), \mathfrak{S}_{2,0}(\xi), \mathfrak{S}_{2,1}(\xi), \mathfrak{S}_{2,2}(\xi), \mathfrak{S}_{2,3}(\xi), \mathfrak{S}_{2,4}(\xi), \mathfrak{S}_{2,5}(\xi)]^T$

$$\mathbb{H}'_{12 \times 12} = \begin{bmatrix} 0 & 0 & \frac{1}{8\sqrt{5}} & 0 & 0 & 0 & 0 & 0 & 0 & 0 & 0 & 0 \\ 0 & 0 & 0 & \frac{1}{8\sqrt{21}} & 0 & 0 & 0 & 0 & 0 & 0 & 0 & 0 \\ 0 & 0 & 0 & 0 & \frac{\sqrt{5}}{144} & 0 & 0 & 0 & 0 & 0 & 0 & 0 \\ 0 & 0 & 0 & 0 & 0 & \frac{\sqrt{7}}{80} & 0 & 0 & 0 & 0 & 0 & 0 \\ 0 & 0 & 0 & 0 & 0 & 0 & 0 & 0 & 0 & 0 & 0 & 0 \\ 0 & 0 & 0 & 0 & 0 & 0 & 0 & 0 & \frac{1}{8\sqrt{5}} & 0 & 0 & 0 \\ 0 & 0 & 0 & 0 & 0 & 0 & 0 & 0 & 0 & \frac{1}{8\sqrt{21}} & 0 & 0 \\ 0 & 0 & 0 & 0 & 0 & 0 & 0 & 0 & 0 & 0 & \frac{\sqrt{5}}{144} & 0 \\ 0 & 0 & 0 & 0 & 0 & 0 & 0 & 0 & 0 & 0 & 0 & \frac{\sqrt{7}}{80} \\ 0 & 0 & 0 & 0 & 0 & 0 & 0 & 0 & 0 & 0 & 0 & 0 \\ 0 & 0 & 0 & 0 & 0 & 0 & 0 & 0 & 0 & 0 & 0 & 0 \end{bmatrix} \quad \bar{\mathfrak{S}}'_{12}(\xi) = \begin{bmatrix} 0 \\ 0 \\ 0 \\ 0 \\ \frac{1}{40\sqrt{13}} \mathfrak{S}_{1,6}(\xi) \\ \frac{\sqrt{13}}{168} \mathfrak{S}_{1,7}(\xi) \\ 0 \\ 0 \\ 0 \\ 0 \\ \frac{1}{40\sqrt{13}} \mathfrak{S}_{2,6}(\xi) \\ \frac{\sqrt{13}}{168} \mathfrak{S}_{2,7}(\xi) \end{bmatrix}$$

Similarly, we can generate matrices for our convenience.

4 Taylor wavelet collocation method

In this part, the TWCM is used to solve a stiff system numerically as a SCODE (1.1).

Consider the subsequent nonlinear stiff system involving two equations of the state:

$$\left. \begin{aligned} y'(\xi) &= F(y(\xi), z(\xi), \xi) \\ z'(\xi) &= G(y(\xi), z(\xi), \xi) \end{aligned} \right\} \tag{4.1}$$

With the primary constraints given by $y(0) = \alpha, z(0) = \beta$.
Assume that,

$$\left. \begin{aligned} y'(\xi) &= A^T \mathfrak{S}(\xi) \\ z'(\xi) &= B^T \mathfrak{S}(\xi) \end{aligned} \right\} \tag{4.2}$$

where, $A^T = [a_{1,0}, \dots, a_{1,M-1}, a_{2,0}, \dots, a_{2,M-1}, a_{2^{k-1},0}, \dots, a_{2^{k-1},M-1}]$,

$$B^T = [b_{1,0}, \dots, b_{1,M-1}, b_{2,0}, \dots, b_{2,M-1}, b_{2^{k-1},0}, \dots, b_{2^{k-1},M-1}]$$

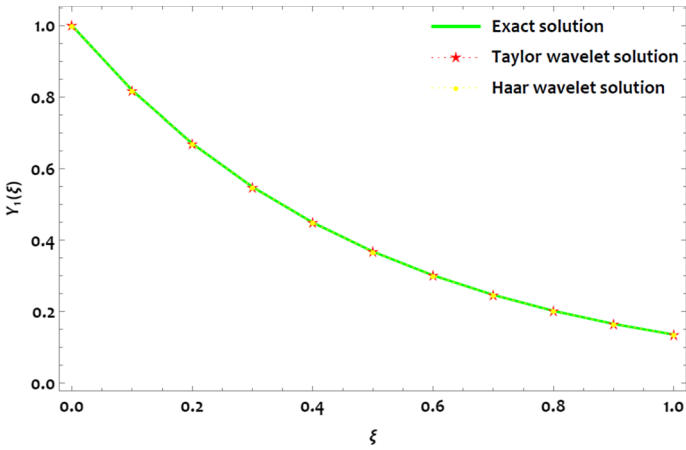


Fig. 1 Visual interpretation of the result $Y_1(\xi)$ of example 1

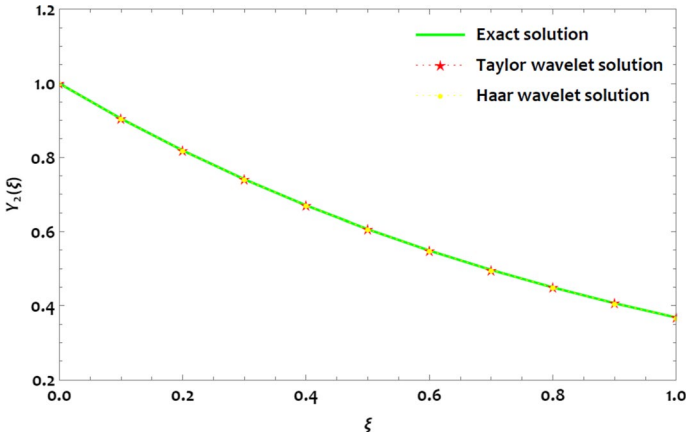


Fig. 2 Visual interpretation of the result $Y_2(\xi)$ of example 1

$$S(\xi) = [S(\xi)_{1,0}, \dots, S(\xi)_{1,M-1}, S(\xi)_{2,0}, \dots, S(\xi)_{2,M-1}, S(\xi)_{2^{k-1},0}, \dots, S(\xi)_{2^{k-1},M-1}]$$

Integrating the Eq. (4.2) regarding ' ξ ' from '0' to ' ξ .' We get.

$$y(\xi) = y(0) + \int_0^\xi A^T S(\xi) d\xi$$

$$z(\xi) = z(0) + \int_0^\xi B^T S(\xi) d\xi$$

Using Eq. (3.1) and primary constraints $y(0) = \alpha$ and $z(0) = \beta$ expressed in terms of $S(\xi)$ by using the linear combination of Taylor wavelets we obtain,

Table 1 Comparison of the solution $Y_1(\xi)$ obtained by TWCM at diverse values of M and k , for example, 1

ξ	Exact solution	Taylor wavelet Method solution	AE of TWCM with ND Solve			
			$k=1, M=6,$		$k=2, M=6$	
			$k=1, M=8$	$k=2, M=8$	$k=1, M=8$	$k=2, M=8$
0	1.000000000000	1.000000000000	0	0	0	0
0.1	0.818730753078	0.818730753071	5.90×10^{-8}	4.03×10^{-9}	2.06×10^{-9}	1.81×10^{-12}
0.2	0.670320046036	0.670320046039	3.48×10^{-7}	2.54×10^{-9}	6.26×10^{-10}	1.21×10^{-12}
0.3	0.548811636094	0.548811636093	3.98×10^{-7}	2.48×10^{-9}	4.84×10^{-10}	1.93×10^{-12}
0.4	0.449328964117	0.449328964118	1.89×10^{-7}	1.70×10^{-9}	4.39×10^{-10}	6.02×10^{-12}
0.5	0.367879441171	0.367879441171	3.43×10^{-7}	8.62×10^{-10}	8.62×10^{-10}	6.44×10^{-13}
0.6	0.301194211912	0.301194211914	1.91×10^{-7}	1.44×10^{-9}	7.09×10^{-10}	8.44×10^{-13}
0.7	0.246596963942	0.246596963939	7.44×10^{-7}	1.01×10^{-9}	6.23×10^{-10}	2.93×10^{-13}
0.8	0.201896517995	0.201896518004	1.43×10^{-6}	9.75×10^{-10}	1.77×10^{-9}	5.87×10^{-13}
0.9	0.165298888222	0.165298888164	1.83×10^{-6}	6.27×10^{-9}	1.83×10^{-8}	2.30×10^{-12}
1.0	0.135335283237	0.135335284409	3.48×10^{-5}	1.46×10^{-7}	2.40×10^{-7}	2.71×10^{-10}

Table 2 Comparison of absolute error for the solution $Y_1(\xi)$ with different methods

ξ	AE of Taylor wavelet with exact solution		AE of Haar wavelet with exact solution	AE of CWCP (N=8) [43]	AE of FWCM (M=8)	AE of ND Solver with exact solution
	k=1, M=10	k=2, M=10				
0	0	0	0	0	0	0
0.1	7.00×10^{-12}	2.22×10^{-15}	8.10×10^{-6}	–	–	4.19×10^{-9}
0.2	3.08×10^{-12}	7.77×10^{-16}	2.91×10^{-6}	0.45×10^{-8}	0.78×10^{-9}	2.06×10^{-9}
0.3	8.95×10^{-13}	9.99×10^{-16}	2.21×10^{-6}	–	–	6.18×10^{-9}
0.4	1.21×10^{-12}	7.49×10^{-15}	1.67×10^{-6}	0.61×10^{-8}	0.33×10^{-9}	8.78×10^{-9}
0.5	6.44×10^{-13}	5.55×10^{-17}	1.25×10^{-6}	–	–	1.02×10^{-8}
0.6	1.50×10^{-12}	9.43×10^{-16}	9.37×10^{-7}	0.10×10^{-8}	0.93×10^{-9}	1.08×10^{-8}
0.7	2.57×10^{-12}	2.77×10^{-16}	6.87×10^{-7}	–	–	1.09×10^{-8}
0.8	9.37×10^{-12}	8.88×10^{-16}	4.99×10^{-7}	0.13×10^{-8}	0.11×10^{-7}	1.06×10^{-8}
0.9	5.74×10^{-11}	2.58×10^{-15}	2.50×10^{-7}	–	–	1.00×10^{-8}
1.0	1.17×10^{-9}	3.16×10^{-13}	1.70×10^{-7}	0.53×10^{-7}	0.13×10^{-5}	9.39×10^{-9}

$$\left. \begin{aligned} y(\xi) &= C^T \mathbb{S}(\xi) + A^T \left[\mathbb{B} \mathbb{S}(\xi) + \bar{\mathbb{S}}(\xi_i) \right] \\ z(\xi) &= E^T \mathbb{S}(\xi) + B^T \left[\mathbb{B} \mathbb{S}(\xi) + \bar{\mathbb{S}}(\xi_i) \right] \end{aligned} \right\} \quad (4.3)$$

where C and E are the known vectors. Now, substitute (4.2) and (4.3) in (4.1), we obtain

$$\left. \begin{aligned} A^T \mathbb{S}(\xi) &= F \left(C^T \mathbb{S}(\xi) + A^T \left[\mathbb{B} \mathbb{S}(\xi) + \bar{\mathbb{S}}(\xi) \right], E^T \mathbb{S}(\xi) + B^T \left[\mathbb{B} \mathbb{S}(\xi) + \bar{\mathbb{S}}(\xi) \right], \xi \right) \\ B^T \mathbb{S}(\xi) &= G \left(C^T \mathbb{S}(\xi) + A^T \left[\mathbb{B} \mathbb{S}(\xi) + \bar{\mathbb{S}}(\xi) \right], E^T \mathbb{S}(\xi) + B^T \left[\mathbb{B} \mathbb{S}(\xi) + \bar{\mathbb{S}}(\xi) \right], \xi \right) \end{aligned} \right\} \quad (4.4)$$

and collocate the obtained equations by the following collocation points $\xi_i = \frac{2i-1}{2^k M}, i = 1, 2 \dots M$.

$$\left. \begin{aligned} A^T \mathbb{S}(\xi_i) &= F \left(C^T \mathbb{S}(\xi_i) + A^T \left[\mathbb{B} \mathbb{S}(\xi_i) + \bar{\mathbb{S}}(\xi_i) \right], E^T \mathbb{S}(\xi_i) + B^T \left[\mathbb{B} \mathbb{S}(\xi_i) + \bar{\mathbb{S}}(\xi_i) \right], \xi_i \right) \\ B^T \mathbb{S}(\xi_i) &= G \left(C^T \mathbb{S}(\xi_i) + A^T \left[\mathbb{B} \mathbb{S}(\xi_i) + \bar{\mathbb{S}}(\xi_i) \right], E^T \mathbb{S}(\xi_i) + B^T \left[\mathbb{B} \mathbb{S}(\xi_i) + \bar{\mathbb{S}}(\xi_i) \right], \xi_i \right) \end{aligned} \right\} \quad (4.5)$$

Let $f_i(\xi_1, \xi_2, \dots, \xi_i) = A^T \mathbb{S}(\xi_i) - F \left(C^T \mathbb{S}(\xi_i) + A^T \left[\mathbb{B} \mathbb{S}(\xi_i) + \bar{\mathbb{S}}(\xi_i) \right], E^T \mathbb{S}(\xi_i) + B^T \left[\mathbb{B} \mathbb{S}(\xi_i) + \bar{\mathbb{S}}(\xi_i) \right], \xi_i \right)$ and $g_i(\xi_1, \xi_2, \dots, \xi_i) = B^T \mathbb{S}(\xi_i) - G \left(C^T \mathbb{S}(\xi_i) + A^T \left[\mathbb{B} \mathbb{S}(\xi_i) + \bar{\mathbb{S}}(\xi_i) \right], E^T \mathbb{S}(\xi_i) + B^T \left[\mathbb{B} \mathbb{S}(\xi_i) + \bar{\mathbb{S}}(\xi_i) \right], \xi_i \right)$

If the components of one iteration $\xi^{(l)} \in \mathbb{R}$ are known as: $\xi_1^{(l)}, \xi_2^{(l)}, \dots, \xi_i^{(l)}$, then, the Taylor expansion of the first equations around these components is given by:

Table 3 Comparison of the solution $Y_2(\xi)$ obtained by TWCM at diverse values of M and k , for example, 1

ξ	Exact solution	Taylor wavelet Method solution	AE of TWCM with exact solution			
			k = 1, M = 6,	k = 2, M = 6	k = 1, M = 8	k = 2, M = 8
0	1.000000000000	1.000000000000	0	0	0	0
0.1	0.904837418036	0.904837509405	9.13×10^{-8}	6.43×10^{-10}	1.79×10^{-10}	3.73×10^{-13}
0.2	0.818730753078	0.818730809543	5.64×10^{-8}	6.39×10^{-10}	1.26×10^{-10}	3.57×10^{-13}
0.3	0.740818220682	0.740818269881	4.91×10^{-8}	5.10×10^{-10}	1.25×10^{-10}	3.30×10^{-13}
0.4	0.670320046036	0.670320097953	5.19×10^{-8}	5.37×10^{-10}	1.10×10^{-10}	3.09×10^{-13}
0.5	0.606530659713	0.606530703769	4.40×10^{-8}	9.96×10^{-11}	9.96×10^{-11}	2.13×10^{-13}
0.6	0.548811636094	0.548811672179	3.60×10^{-8}	4.66×10^{-10}	9.26×10^{-11}	3.92×10^{-13}
0.7	0.496585303791	0.496585343198	3.94×10^{-8}	4.56×10^{-10}	7.86×10^{-11}	3.65×10^{-13}
0.8	0.449328964117	0.449329000288	3.61×10^{-8}	3.72×10^{-10}	8.07×10^{-11}	3.34×10^{-13}
0.9	0.406569659741	0.406569666601	6.86×10^{-9}	3.77×10^{-10}	5.85×10^{-11}	3.09×10^{-13}
1.0	0.367879441171	0.367879509180	6.80×10^{-8}	6.12×10^{-10}	1.65×10^{-11}	2.35×10^{-13}

Table 4 Comparison of absolute error for the solution $Y_2(\xi)$ with different methods

ξ	AE of Taylor wavelet with exact solution		AE of Haar wavelet with exact solution	AE of CMCP (N=8) [43]	AE of FWCM (M=8)	AE of ND Solver with exact solution
	k=1, M=10	k=2, M=10				
0	0	0	0	0	0	0
0.1	3.40×10^{-13}	1.10×10^{-16}	–	–	–	2.18×10^{-9}
0.2	2.81×10^{-13}	2.22×10^{-16}	0.14×10^{-10}	0.14×10^{-10}	0.44×10^{-10}	1.38×10^{-9}
0.3	2.60×10^{-13}	2.22×10^{-16}	–	–	–	4.30×10^{-9}
0.4	2.33×10^{-13}	1.11×10^{-16}	0.21×10^{-10}	0.21×10^{-10}	0.37×10^{-10}	6.65×10^{-9}
0.5	2.13×10^{-13}	2.22×10^{-16}	–	–	–	8.51×10^{-9}
0.6	1.90×10^{-13}	2.22×10^{-16}	0.22×10^{-10}	0.22×10^{-10}	0.31×10^{-10}	9.97×10^{-9}
0.7	1.75×10^{-13}	3.33×10^{-16}	–	–	–	1.10×10^{-8}
0.8	1.50×10^{-13}	3.88×10^{-16}	0.18×10^{-10}	0.18×10^{-10}	0.15×10^{-10}	1.18×10^{-8}
0.9	1.82×10^{-13}	3.88×10^{-16}	–	–	–	1.24×10^{-8}
1.0	7.08×10^{-13}	1.66×10^{-16}	0.20×10^{-10}	0.20×10^{-10}	0.38×10^{-9}	1.28×10^{-8}

$$f_1(\xi_1^{(l+1)}, \xi_2^{(l+1)}, \dots, \xi_i^{(l+1)}) = f(\xi_1^{(l)}, \xi_2^{(l)}, \dots, \xi_i^{(l)}) + \left. \frac{\partial f_1}{\partial \xi_1} \right|_{\xi^{(l)}} (\xi_1^{(l+1)} - \xi_1^{(l)}) + \left. \frac{\partial f_1}{\partial \xi_2} \right|_{\xi^{(l)}} (\xi_2^{(l+1)} - \xi_2^{(l)}) + (\xi_i^{(l+1)} - \xi_i^{(l)})$$

and

$$g_1(\xi_1^{(l+1)}, \xi_2^{(l+1)}, \dots, \xi_i^{(l+1)}) = g(\xi_1^{(l)}, \xi_2^{(l)}, \dots, \xi_i^{(l)}) + \left. \frac{\partial g_1}{\partial \xi_1} \right|_{\xi^{(l)}} (\xi_1^{(l+1)} - \xi_1^{(l)}) + \left. \frac{\partial g_1}{\partial \xi_2} \right|_{\xi^{(l)}} (\xi_2^{(l+1)} - \xi_2^{(l)}) + \left. \frac{\partial g}{\partial \xi_i} \right|_{\xi^{(l)}} (\xi_i^{(l+1)} - \xi_i^{(l)})$$

Applying the Taylor expansion in the same manner for f_2, f_3, \dots, f_i and g_1, g_3, \dots, g_i , we obtained the following system of linear equations, with the unknown being the components of the vector $\xi^{(l+1)}$:

$$\begin{pmatrix} f_1(\xi^{(l+1)}) \\ f_2(\xi^{(l+1)}) \\ \vdots \\ f_i(\xi^{(l+1)}) \end{pmatrix} = \begin{pmatrix} f_1(\xi^{(l)}) \\ f_2(\xi^{(l)}) \\ \vdots \\ f_i(\xi^{(l)}) \end{pmatrix} + \begin{pmatrix} \left. \frac{\partial f_1}{\partial \xi_1} \right|_{\xi^{(l)}} & \left. \frac{\partial f_1}{\partial \xi_2} \right|_{\xi^{(l)}} & \dots & \left. \frac{\partial f_1}{\partial \xi_i} \right|_{\xi^{(l)}} \\ \left. \frac{\partial f_2}{\partial \xi_1} \right|_{\xi^{(l)}} & \left. \frac{\partial f_2}{\partial \xi_2} \right|_{\xi^{(l)}} & \dots & \left. \frac{\partial f_2}{\partial \xi_i} \right|_{\xi^{(l)}} \\ \vdots & \vdots & \ddots & \vdots \\ \left. \frac{\partial f_i}{\partial \xi_1} \right|_{\xi^{(l)}} & \left. \frac{\partial f_i}{\partial \xi_2} \right|_{\xi^{(l)}} & \dots & \left. \frac{\partial f_i}{\partial \xi_i} \right|_{\xi^{(l)}} \end{pmatrix} \begin{pmatrix} (\xi_1^{(l+1)} - \xi_1^{(l)}) \\ (\xi_2^{(l+1)} - \xi_2^{(l)}) \\ \vdots \\ (\xi_i^{(l+1)} - \xi_i^{(l)}) \end{pmatrix} \text{ and}$$

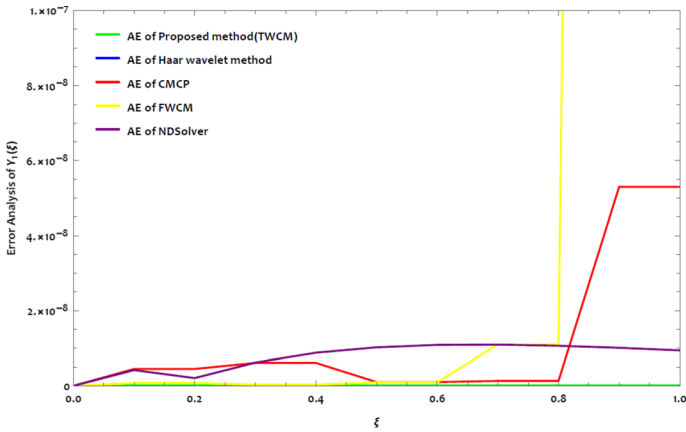


Fig. 3 Comparison of AE of the result $Y_1(\xi)$ with different techniques, for example, 1

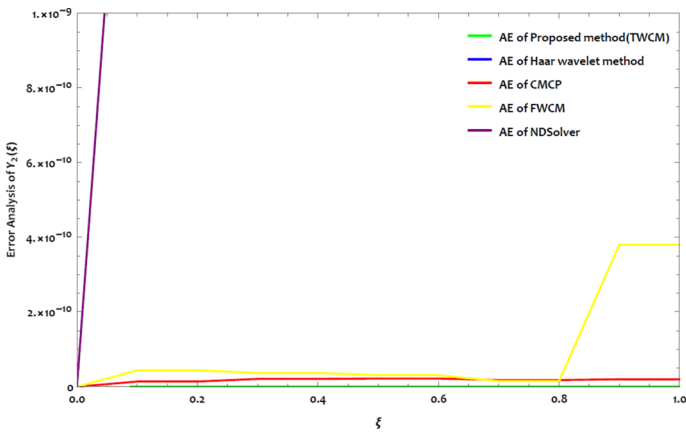


Fig. 4 Comparison of AE of the result $Y_2(\xi)$ with different techniques, for example, 1

$$\begin{pmatrix} g_1(\xi^{(l+1)}) \\ g_2(\xi^{(l+1)}) \\ \vdots \\ g_i(\xi^{(l+1)}) \end{pmatrix} = \begin{pmatrix} g_1(\xi^{(i)}) \\ g_2(\xi^{(i)}) \\ \vdots \\ g_i(\xi^{(i)}) \end{pmatrix} + \begin{pmatrix} \frac{\partial g_1}{\partial \xi_1} \Big|_{\xi^{(l)}} & \frac{\partial g_1}{\partial \xi_2} \Big|_{\xi^{(l)}} & \dots & \frac{\partial g_1}{\partial \xi_i} \Big|_{\xi^{(l)}} \\ \frac{\partial g_2}{\partial \xi_1} \Big|_{\xi^{(l)}} & \frac{\partial g_2}{\partial \xi_2} \Big|_{\xi^{(l)}} & \dots & \frac{\partial g_2}{\partial \xi_i} \Big|_{\xi^{(l)}} \\ \vdots & \vdots & \ddots & \vdots \\ \frac{\partial g_i}{\partial \xi_1} \Big|_{\xi^{(l)}} & \frac{\partial g_i}{\partial \xi_2} \Big|_{\xi^{(l)}} & \dots & \frac{\partial g_i}{\partial \xi_i} \Big|_{\xi^{(l)}} \end{pmatrix} \begin{pmatrix} \xi_1^{(l+1)} - \xi_1^{(l)} \\ \xi_2^{(l+1)} - \xi_2^{(l)} \\ \vdots \\ \xi_i^{(l+1)} - \xi_i^{(l)} \end{pmatrix}$$

By setting the left-hand side to zero (which is desired value for the functions f_2, f_3, \dots, f_i and g_1, g_3, \dots, g_i) then, the system can write as:

Table 6 Comparison of absolute error for the solution $P(\xi)$ with different methods

ξ	AE of Taylor wavelet with exact solution		AE of Haar wavelet with exact solution	AE of ND Solver with exact solution
	$k = 1, M = 10$	$k = 2, M = 10$		
0	0	0	0	0
0.1	8.39×10^{-11}	5.92×10^{-14}	2.54×10^{-6}	2.20×10^{-8}
0.2	8.82×10^{-11}	6.58×10^{-14}	2.13×10^{-6}	6.62×10^{-8}
0.3	9.81×10^{-11}	7.27×10^{-14}	1.82×10^{-6}	6.08×10^{-9}
0.4	1.08×10^{-10}	8.07×10^{-14}	1.59×10^{-6}	3.36×10^{-8}
0.5	1.19×10^{-10}	2.16×10^{-14}	1.43×10^{-6}	6.26×10^{-8}
0.6	1.32×10^{-10}	4.58×10^{-14}	1.32×10^{-6}	5.24×10^{-8}
0.7	1.46×10^{-10}	5.07×10^{-14}	1.25×10^{-6}	2.41×10^{-8}
0.8	1.61×10^{-10}	5.61×10^{-14}	1.22×10^{-6}	4.61×10^{-8}
0.9	1.75×10^{-10}	6.21×10^{-14}	1.23×10^{-6}	6.56×10^{-9}
1.0	2.52×10^{-9}	8.58×10^{-14}	1.26×10^{-6}	3.42×10^{-8}

$$\begin{pmatrix} \left. \frac{\partial f_1}{\partial \xi_1} \right|_{\xi^{(l)}} & \left. \frac{\partial f_1}{\partial \xi_2} \right|_{\xi^{(l)}} & \cdots & \left. \frac{\partial f_1}{\partial \xi_i} \right|_{\xi^{(l)}} \\ \left. \frac{\partial f_2}{\partial \xi_1} \right|_{\xi^{(l)}} & \left. \frac{\partial f_2}{\partial \xi_2} \right|_{\xi^{(l)}} & \cdots & \left. \frac{\partial f_2}{\partial \xi_i} \right|_{\xi^{(l)}} \\ \vdots & \vdots & \vdots & \vdots \\ \left. \frac{\partial f_i}{\partial \xi_1} \right|_{\xi^{(l)}} & \left. \frac{\partial f_i}{\partial \xi_2} \right|_{\xi^{(l)}} & \cdots & \left. \frac{\partial f_i}{\partial \xi_i} \right|_{\xi^{(l)}} \end{pmatrix} \begin{pmatrix} \left(\xi_1^{(l+1)} - \xi_1^{(l)} \right) \\ \left(\xi_2^{(l+1)} - \xi_2^{(l)} \right) \\ \vdots \\ \left(\xi_i^{(l+1)} - \xi_i^{(l)} \right) \end{pmatrix} = - \begin{pmatrix} f_1(\xi^{(i)}) \\ f_2(\xi^{(i)}) \\ \vdots \\ f_i(\xi^{(i)}) \end{pmatrix} \tag{4.6}$$

$$\begin{pmatrix} \left. \frac{\partial g_1}{\partial \xi_1} \right|_{\xi^{(l)}} & \left. \frac{\partial g_1}{\partial \xi_2} \right|_{\xi^{(l)}} & \cdots & \left. \frac{\partial g_1}{\partial \xi_i} \right|_{\xi^{(l)}} \\ \left. \frac{\partial g_2}{\partial \xi_1} \right|_{\xi^{(l)}} & \left. \frac{\partial g_2}{\partial \xi_2} \right|_{\xi^{(l)}} & \cdots & \left. \frac{\partial g_2}{\partial \xi_i} \right|_{\xi^{(l)}} \\ \vdots & \vdots & \vdots & \vdots \\ \left. \frac{\partial g_i}{\partial \xi_1} \right|_{\xi^{(l)}} & \left. \frac{\partial g_i}{\partial \xi_2} \right|_{\xi^{(l)}} & \cdots & \left. \frac{\partial g_i}{\partial \xi_i} \right|_{\xi^{(l)}} \end{pmatrix} \begin{pmatrix} \left(\xi_1^{(l+1)} - \xi_1^{(l)} \right) \\ \left(\xi_2^{(l+1)} - \xi_2^{(l)} \right) \\ \vdots \\ \left(\xi_i^{(l+1)} - \xi_i^{(l)} \right) \end{pmatrix} = - \begin{pmatrix} g_1(\xi^{(i)}) \\ g_2(\xi^{(i)}) \\ \vdots \\ g_i(\xi^{(i)}) \end{pmatrix} \tag{4.7}$$

Setting $K = \left. \frac{\partial f_i}{\partial \xi_j} \right|_{\xi^{(l)}}$ and $J = \left. \frac{\partial g_i}{\partial \xi_j} \right|_{\xi^{(l)}}$, where K and J are Jacobian matrices for the above systems. Then, the above system can be written in matrix form as follows:

$$\left. \begin{aligned} K\Delta x &= -f \\ J\Delta x &= -g \end{aligned} \right\}$$

where K and J are $i \times i$ matrices, $-f$ and $-g$ are vectors of n components, and Δx is an n - dimensional vector with the components $\left(\xi_1^{(l+1)} - \xi_1^{(l)} \right), \left(\xi_2^{(l+1)} - \xi_2^{(l)} \right), \left(\xi_i^{(l+1)} - \xi_i^{(l)} \right)$.

Table 7 Comparison of the solution $Q(\xi)$ obtained by TWCM at diverse values of M and k , for example, 2

ξ	Exact solution	Taylor wavelet Method solution	AE of TWCM with exact solution				
			$k = 1, M = 6,$	$k = 2, M = 6$	$k = 1, M = 8$	$k = 2, M = 8$	$k = 1, M = 10$
0	1.000000000000	1.000000000000	0	0	0	0	0
0.1	0.904837418036	0.904837502236	8.42×10^{-8}	5.79×10^{-10}	1.33×10^{-10}	2.66×10^{-13}	1.44×10^{-13}
0.2	0.818730753078	0.818730804802	5.17×10^{-8}	5.81×10^{-10}	9.54×10^{-11}	2.52×10^{-13}	1.22×10^{-13}
0.3	0.740818220682	0.740818266403	4.57×10^{-8}	4.64×10^{-10}	9.45×10^{-10}	2.32×10^{-13}	1.12×10^{-13}
0.4	0.670320046036	0.670320094102	4.80×10^{-8}	4.72×10^{-10}	8.24×10^{-10}	2.24×10^{-13}	1.01×10^{-13}
0.5	0.606530659713	0.606530700028	4.03×10^{-8}	7.54×10^{-11}	7.54×10^{-10}	9.17×10^{-14}	9.17×10^{-13}
0.6	0.548811636094	0.548811669538	3.34×10^{-8}	4.18×10^{-10}	6.90×10^{-10}	2.44×10^{-13}	8.29×10^{-13}
0.7	0.496585303791	0.496585340858	3.70×10^{-8}	4.14×10^{-10}	1.33×10^{-10}	2.28×10^{-13}	7.47×10^{-13}
0.8	0.449328964117	0.449328996175	3.20×10^{-8}	3.37×10^{-10}	1.33×10^{-10}	2.09×10^{-13}	6.90×10^{-13}
0.9	0.406569659741	0.406569664197	4.45×10^{-9}	3.36×10^{-10}	1.33×10^{-10}	1.97×10^{-13}	5.38×10^{-13}
1.0	0.367879441171	0.367879534178	9.30×10^{-8}	7.04×10^{-10}	1.33×10^{-10}	3.60×10^{-13}	2.07×10^{-13}

Table 8 Comparison of absolute error for the solution $Q(\xi)$ with different methods

ξ	AE of Taylor wavelet with exact solution		AE of Haar wavelet with exact solution	AE of ND Solver with exact solution
	$k=1, M=10$	$k=2, M=10$		
0	0	0	0	0
0.1	8.39×10^{-11}	5.92×10^{-14}	1.61×10^{-6}	1.16×10^{-8}
0.2	8.82×10^{-11}	6.58×10^{-14}	1.35×10^{-6}	4.92×10^{-8}
0.3	9.81×10^{-11}	7.27×10^{-14}	1.13×10^{-6}	4.07×10^{-9}
0.4	1.08×10^{-10}	8.07×10^{-14}	1.13×10^{-6}	8.95×10^{-9}
0.5	1.19×10^{-10}	2.16×10^{-14}	9.37×10^{-7}	2.57×10^{-8}
0.6	1.32×10^{-10}	4.58×10^{-14}	7.71×10^{-7}	2.14×10^{-8}
0.7	1.46×10^{-10}	5.07×10^{-14}	6.28×10^{-7}	3.71×10^{-9}
0.8	1.61×10^{-10}	5.61×10^{-14}	5.05×10^{-7}	2.65×10^{-8}
0.9	1.75×10^{-10}	6.21×10^{-14}	3.99×10^{-7}	6.17×10^{-9}
1.0	2.52×10^{-9}	8.58×10^{-14}	3.10×10^{-7}	4.53×10^{-9}

Combining the above two systems of equations, we obtain $Q\Delta x = -p$, Where $Q = K + L$ and $p = f + g$. If Q is invertible, then the above system can be solved as follows:

$$\Delta x = -Q^{-1}p \Rightarrow \xi^{(l+1)} = \xi^{(l)} - K^{-1}p$$

which provides the values of unknown Taylor wavelet coefficients. Substitute these coefficient values in (4.3) yields the TWCM numerical solution for the system.

5 Numerical results and discussion

Here, we considered a few examples to demonstrate the proposed method and outcomes are computed using the symbolic calculus programming language Mathematica.

Example 1: Let us consider the nonlinear stiff system of the form: [42]

$$\left. \begin{aligned} \frac{dY_1(\xi)}{d\xi} &= -1002Y_1(\xi) + 1000Y_2^2(\xi) \\ \frac{dY_2(\xi)}{d\xi} &= Y_1(\xi) - Y_2(\xi)(1 + Y_2(\xi)) \end{aligned} \right\} \quad (5.1)$$

The given initial condition are: $Y_1(0) = 1, Y_2(0) = 1$. The exact solutions to the stiff chemical problem are $Y_1(\xi) = e^{-2\xi}$ and $Y_2(\xi) = e^\xi$. The Taylor wavelet collocation method (TWCM) solutions, for example, 1, are shown in Figs. 1, 2, revealing that the proposed method solutions are reasonably close to the exact solution compared to existing methods such as Chebyshev polynomials (CMCP), Fibonacci

Table 5 Comparison of the solution $P(\xi)$ obtained by TWCM at diverse values of M and k , for example, 2

ξ	Exact solution	Taylor wavelet	AE of TWCM with exact solution			
			$k = 1, M = 6,$	$k = 2, M = 6$	$k = 1, M = 8$	$k = 2, M = 8$
0	-0.333333333333	-0.333333333333	0	0	0	0
0.1	-0.272910251026	-0.272913387007	3.13×10^{-6}	2.69×10^{-8}	1.96×10^{-8}	4.78×10^{-11}
0.2	-0.223440015345	-0.223442645502	2.63×10^{-6}	3.16×10^{-8}	1.82×10^{-8}	5.50×10^{-11}
0.3	-0.182937212031	-0.182940060813	2.84×10^{-6}	3.25×10^{-8}	2.11×10^{-8}	6.13×10^{-11}
0.4	-0.149776321372	-0.149779672838,	3.35×10^{-6}	3.79×10^{-8}	2.29×10^{-8}	6.94×10^{-11}
0.5	-0.122626480392	-0.122630089668	3.60×10^{-6}	2.54×10^{-8}	2.54×10^{-8}	1.19×10^{-10}
0.6	-0.100398070637	-0.100401964399	3.89×10^{-6}	3.80×10^{-8}	2.82×10^{-8}	1.49×10^{-10}
0.7	-0.082198987980	-0.0822034684517	4.48×10^{-6}	4.27×10^{-8}	3.08×10^{-8}	1.66×10^{-10}
0.8	-0.067298839331	-0.0673037614108	4.92×10^{-6}	4.63×10^{-8}	3.49×10^{-8}	1.84×10^{-10}
0.9	-0.055099629407	-0.0551044573745	4.82×10^{-6}	5.19×10^{-8}	3.60×10^{-8}	2.04×10^{-10}
1.0	-0.045111761078	-0.0451190878232	7.32×10^{-6}	6.44×10^{-8}	5.29×10^{-8}	2.38×10^{-10}

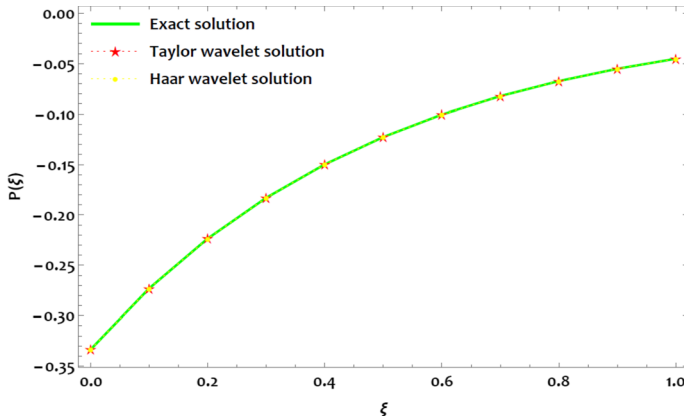


Fig. 5 Plot of the result $P(\xi)$ of example 2

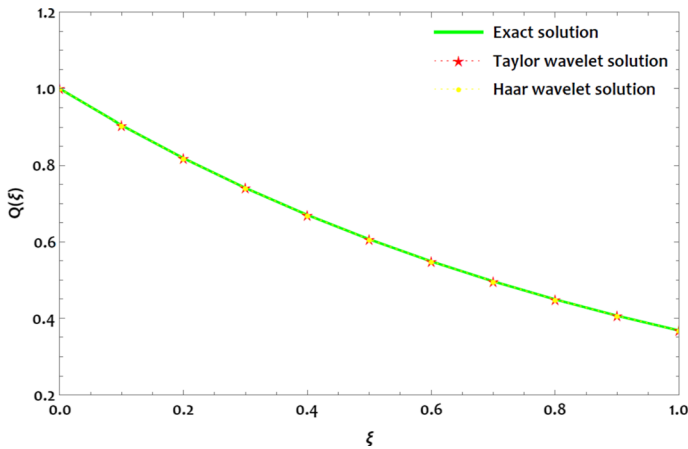


Fig. 6 Plot of the result $Q(\xi)$ of example 2

wavelet collocation method (FWCM), Haar wavelet method and ND Solver. Numerical approximations obtained by the developed technique called TWCM and other current methods are compared with the exact solution. They are tabulated in Tables 1, 2, 3, and 4, and absolute errors of the developed approach with the exact solution are tabulated in Tables 1 and 3. It reveals that the errors obtained by the proposed method are better than those obtained using other existing techniques. TWCM solutions are calculated at diverse values of M and k . Also, by increasing the M and k , we get further precision in the result, which can be seen in Tables 1 and 3. It shows that increasing M and k can obtain a higher-order accuracy. Figures 1, 2, 3, and 4 depict all the graphical representations of numerical simulations and absolute error analysis. From the tables and graphs, it is clear that the TWCM

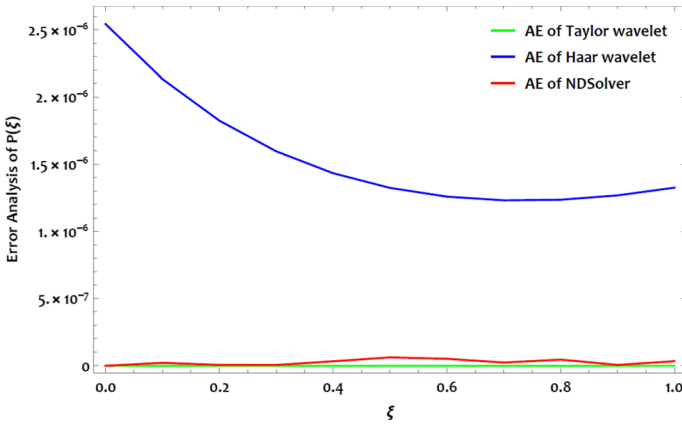


Fig. 7 AE comparison of the result $P(\xi)$ with different techniques, for example, 2

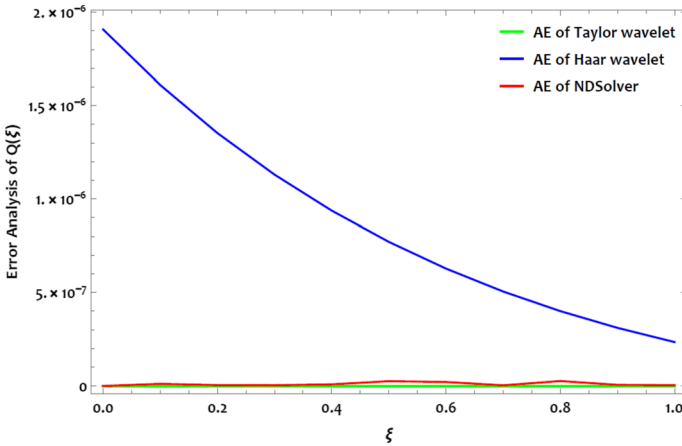


Fig. 8 Judgement of AE of the result $Q(\xi)$ with different techniques, for example, 2

method dominates all the other techniques in obtaining the numerical approximation and yields a satisfactory result for the desired system.

Example 2: Let us consider the following nonlinear stiff chemical problem of the form: [42]

$$\left. \begin{aligned} P'(\xi) &= \delta P(\xi) + Q^2(\xi) \\ Q'(\xi) &= -Q(\xi) \end{aligned} \right\} \tag{5.2}$$

with the given initial condition are: $P(0) = -\frac{1}{\delta+2}$, $Q(0) = 1$. The exact solutions to the stiff chemical problem are $P(\xi) = \frac{e^{-2\xi}}{\delta+2}$ and $Q(\xi) = e^{-\xi}$. The TWCM solutions are shown in Tables 5, 6, 7, and 8 and Figs. 5 and 6, revealing that the proposed

Table 9 Comparison of the solution $Z_1(\xi)$ obtained by TWCM at diverse values of M and k , for example, 3

ξ	Exact solution	Taylor wavelet	AE of TWCM with exact solution				
			k = 1, M = 6	k = 2, M = 6	k = 1, M = 8	k = 2, M = 8	
0			0	0	0	0	k = 1, M = 10
0.1	0.904837418036	0.904837418036	5.68×10^{-8}	3.80×10^{-10}	9.02×10^{-11}	1.84×10^{-13}	9.78×10^{-14}
0.2	0.818730753078	0.818730753078	1.24×10^{-8}	2.62×10^{-10}	3.11×10^{-11}	1.12×10^{-13}	4.95×10^{-14}
0.3	0.740818220682	0.740818220682	2.65×10^{-9}	3.72×10^{-11}	1.04×10^{-11}	4.20×10^{-14}	1.43×10^{-14}
0.4	0.670320046036	0.670320046036	8.74×10^{-9}	4.57×10^{-11}	1.74×10^{-11}	6.77×10^{-15}	1.58×10^{-14}
0.5	0.606530659713	0.606530659713	2.26×10^{-8}	3.55×10^{-11}	3.55×10^{-11}	3.99×10^{-14}	3.99×10^{-14}
0.6	0.548811636094	0.548811636094	3.23×10^{-8}	1.81×10^{-10}	4.91×10^{-11}	5.38×10^{-14}	5.73×10^{-14}
0.7	0.496585303791	0.496585303791	2.93×10^{-8}	9.99×10^{-11}	6.13×10^{-11}	1.27×10^{-15}	6.97×10^{-14}
0.8	0.449328964117	0.449328964117	3.45×10^{-8}	4.13×10^{-11}	5.76×10^{-11}	5.05×10^{-14}	7.49×10^{-14}
0.9	0.406569659741	0.406569659741	6.01×10^{-8}	9.29×10^{-11}	8.78×10^{-11}	8.22×10^{-14}	8.69×10^{-14}
1.0	0.367879441171	0.367879441172	4.50×10^{-8}	2.79×10^{-10}	7.70×10^{-11}	8.06×10^{-14}	8.90×10^{-14}

Table 10 Comparison of absolute error for the solution $Z_1(\xi)$ with different methods

ξ	AE of Taylor wavelet with exact solution		AE of haar wavelet with exact solution	AE of ND Solver with exact solution
	$k=1, M=10$	$k=2, M=10$		
0	0	0	0	0
0.1	9.78×10^{-14}	1.11×10^{-16}	1.24×10^{-6}	2.33×10^{-8}
0.2	4.95×10^{-14}	2.22×10^{-16}	6.68×10^{-6}	9.25×10^{-9}
0.3	1.43×10^{-14}	1.11×10^{-16}	1.84×10^{-7}	2.11×10^{-8}
0.4	1.58×10^{-14}	0	2.02×10^{-7}	3.06×10^{-9}
0.5	3.99×10^{-14}	1.11×10^{-16}	4.95×10^{-7}	1.01×10^{-8}
0.6	5.73×10^{-14}	0	6.99×10^{-7}	6.85×10^{-8}
0.7	6.97×10^{-14}	1.11×10^{-16}	8.21×10^{-7}	8.07×10^{-8}
0.8	7.49×10^{-14}	1.66×10^{-16}	8.73×10^{-7}	7.87×10^{-8}
0.9	8.69×10^{-14}	2.22×10^{-16}	8.65×10^{-7}	3.13×10^{-9}
1.0	8.90×10^{-14}	1.66×10^{-16}	8.11×10^{-7}	9.16×10^{-8}

method solutions are reasonably close to the exact solution compared to the current scheme, such as the Haar wavelet collocation method and ND Solver. Numerical approximations and absolute errors of the developed approach with the exact solution are tabulated in Tables 5, 6, 7, and 8. It is evident from Figs. 5, 6, 7 and 8 that the approximations obtained from TWCM come closer and closer to the exact solution. The errors obtained using the proposed method are better than other existing techniques. TWCM solutions are calculated at diverse values of M and k . Also, by increasing the values of M and k , we get more accuracy in the solution, which can be seen in Tables 5 and 7. It shows that increasing M and k can obtain a higher-order accuracy. Figures 5, 6, 7, and 8 depict all the graphical representations of numerical simulations and absolute error analysis. From the tables and graphs, it is clear that the TWCM dominates all the other techniques in obtaining the numerical approximation and yields a satisfactory result for the desired system.

Example 3: Let us consider the following nonlinear stiff chemical problem of the form: [42]

$$\left. \begin{aligned} Z_1'(\xi) &= -\alpha Z_1(\xi) - \beta Z_2(\xi) + (\alpha + \beta - 1)e^{-\xi} \\ Z_2'(\xi) &= -\beta Z_1(\xi) - \alpha Z_2(\xi) + (\alpha - \beta - 1)e^{-\xi} \end{aligned} \right\} \quad (5.3)$$

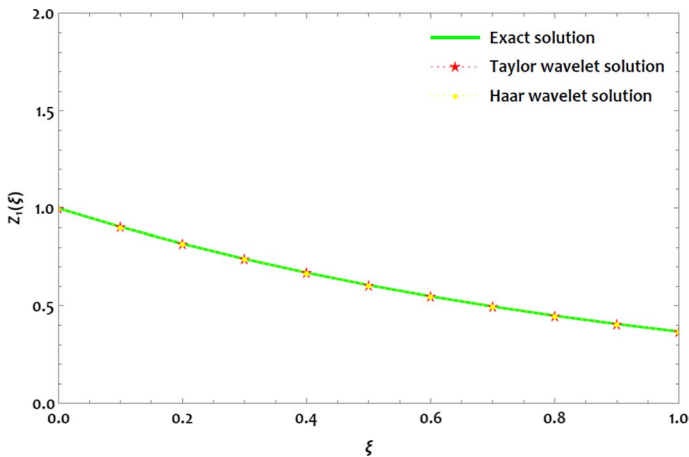
The given initial condition are: $Z_1(0) = 1, Z_2(0) = 1$. The numerical and exact solutions are compared for various values of ξ , and the absolute error between the analytical and approximative solutions at different resolutions (various k and M) is presented in Tables 9 and 11. Tables 10 and 12 provide the comparison of absolute errors of the TWCM with other methods, such as the Haar wavelet collocation method (HWCM) and the ND Solve method. Figures 9 and 10 provide

Table 11 Comparison of the solution $Z_2(\xi)$ obtained by TWCM at diverse values of M and k , for example, 3

ξ	Exact solution	Taylor wavelet	AE of TWCM with exact solution			
			$k=1, M=6,$	$k=2, M=6$	$k=1, M=8$	$k=2, M=8$
0			0	0	0	0
0.1	0.904837418036	0.904837418036	1.04×10^{-7}	7.32×10^{-10}	1.66×10^{-10}	3.29×10^{-13}
0.2	0.818730753078	0.818730753078	7.43×10^{-8}	7.76×10^{-10}	1.33×10^{-10}	3.40×10^{-13}
0.3	0.740818220682	0.740818220682	6.65×10^{-8}	6.68×10^{-10}	1.33×10^{-10}	3.26×10^{-13}
0.4	0.670320046036	0.670320046036	6.60×10^{-8}	6.60×10^{-10}	1.16×10^{-10}	3.09×10^{-13}
0.5	0.606530659713	0.606530659713	5.37×10^{-8}	1.01×10^{-10}	1.01×10^{-10}	1.23×10^{-13}
0.6	0.548811636094	0.548811636094	4.02×10^{-8}	5.27×10^{-10}	8.41×10^{-11}	3.02×10^{-13}
0.7	0.496585303791	0.496585303791	3.67×10^{-8}	5.35×10^{-10}	6.25×10^{-11}	2.86×10^{-13}
0.8	0.449328964117	0.449328964117	2.62×10^{-8}	4.52×10^{-10}	5.28×10^{-11}	2.56×10^{-13}
0.9	0.406569659741	0.406569659741	6.98×10^{-9}	4.30×10^{-10}	1.09×10^{-11}	2.26×10^{-13}
1.0	0.367879441171	0.367879441172	6.30×10^{-8}	7.25×10^{-10}	1.25×10^{-10}	3.54×10^{-13}

Table 12 Comparison of absolute error for the solution $Z_2(\xi)$ with different methods

ξ	AE of Taylor wavelet with exact solution		AE of Haar wavelet with Exact solution	AE of ND Solver with exact solution
	$k=1, M=10$	$k=2, M=10$		
0	0	0	0	0
0.1	1.79×10^{-13}	2.22×10^{-16}	1.90×10^{-6}	3.09×10^{-8}
0.2	1.67×10^{-13}	2.22×10^{-16}	1.80×10^{-6}	2.38×10^{-8}
0.3	1.58×10^{-13}	1.11×10^{-16}	1.61×10^{-6}	3.68×10^{-9}
0.4	1.42×10^{-13}	0	1.37×10^{-6}	2.10×10^{-8}
0.5	1.23×10^{-13}	4.44×10^{-16}	1.09×10^{-6}	1.46×10^{-8}
0.6	1.02×10^{-13}	3.33×10^{-16}	8.07×10^{-7}	4.17×10^{-8}
0.7	8.06×10^{-13}	4.99×10^{-16}	5.21×10^{-7}	5.08×10^{-8}
0.8	6.01×10^{-13}	3.88×10^{-16}	2.52×10^{-7}	4.34×10^{-8}
0.9	3.20×10^{-13}	2.77×10^{-16}	1.00×10^{-8}	8.86×10^{-9}
1.0	1.57×10^{-13}	2.77×10^{-16}	1.97×10^{-7}	3.29×10^{-8}

**Fig. 9** Plot of the solution $Z_1(\xi)$ of example 3

the visual representation of the obtained solution by TWCM compared with other methods. The graphical representation of the absolute error of our suggested approach is carried out in Fig. 11 and 12. Tables and graphs confirm that by simply raising the k and M values, our suggested approach can generate more precise results. The findings shown in the tables and figures demonstrate the suggested approach's superior accuracy over the current numerical models. The tables and graphs show that the proposed approach converges more rapidly with the exact

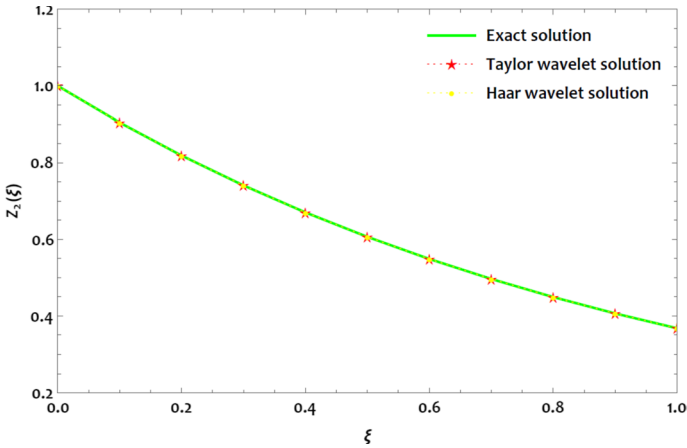


Fig. 10 Plot of the solution $Z_2(\xi)$ of example 3

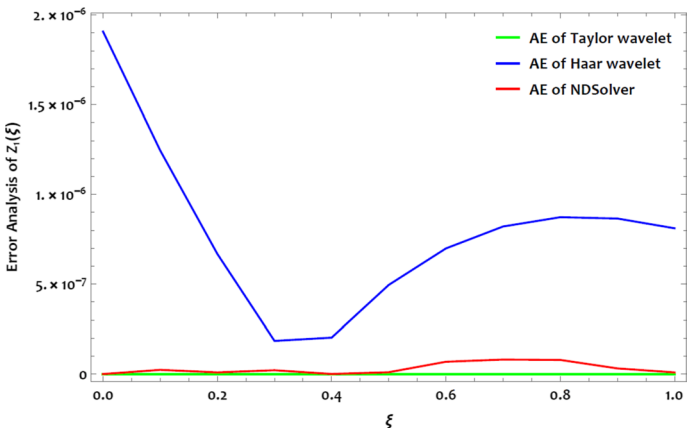


Fig. 11 Comparison of AE of the solution $Z_1(\xi)$ with different techniques, for example 3

values than other methods, and the proposed method is a suitable and powerful tool to solve the above type of stiff chemical problem.

Example 4: Let us consider the following nonlinear stiff nuclear reactor model: [10]

$$\left. \begin{aligned} Z_1'(\xi) &= 0.01 - (0.01 + Z_1(\xi) + Z_2(\xi))(1 + (Z_1(\xi) + 1000)(Z_1(\xi) + 1)) \\ Z_2'(\xi) &= 0.01 - (0.01 + Z_1(\xi) + Z_2(\xi))(1 + Z_1(\xi)^2) \end{aligned} \right\} (5.4)$$

The given initial condition are: $Z_1(0) = 0, Z_2(0) = 0$. This problem has no exact solution. We have solved this model with the Taylor wavelet collocation method at

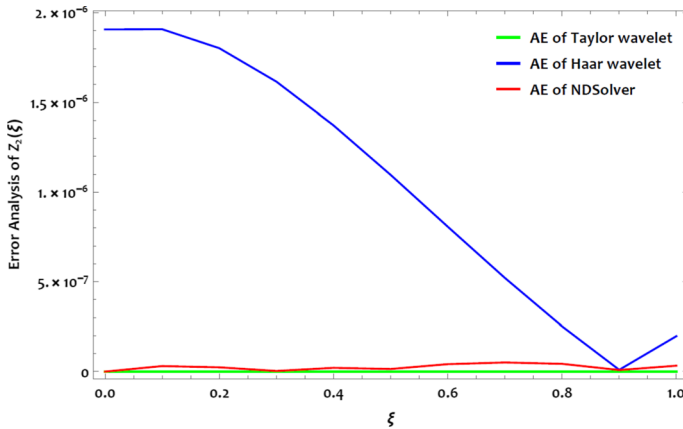


Fig. 12 Comparison of AE of the solution $Z_2(\xi)$ with different techniques, for example, 3

$M=6,7$ and $k=1,2$. Numerical approximations obtained from the TWCM and ND solve are tabulated in Tables 13 and 14 for $Z_1(\xi)$ and $Z_2(\xi)$, respectively. Also, the absolute error computed at different values of k and with the ND solve method (due to the non-availability of the exact solution for the model) are tabulated in the same tables. The numerical approximations are computed with the Haar wavelet collocation method, and the solutions are compared with the ND Solve method and the absolute error of the Haar method is also tabulated in Tables 13 and 14. The graphical representation of the solution $Z_1(\xi)$ and $Z_2(\xi)$ are carried out in Figs. 13 and 14. Also, a graphical representation of the absolute errors is drawn in Figs. 15 and 16. It is easy to see that the errors obtained using the proposed method are lesser than those obtained using the Haar wavelet method. Observing all the above-listed tables and graphs, one can conclude that the developed technique solutions are reasonably close to the ND Solve solution compared to the Haar wavelet collocation method. TWCM solutions are calculated at diverse values of M and k . Tables 13 and 14 reveal that after some stage (M) solution will remain the same; that is, the solution remains stable (never changes by increasing the values of M). The ND Solve solution and the TWCM solution are incredibly similar. Tables and Graphs confirm the above statement. It suggests that TWCM is a suitable method to solve the stiff models.

6 Conclusion

In the present study, we used the Taylor wavelet collocation method (TWCM), which is not stiffness-sensitive and is used to analyze typical nonlinear systems originating in nonlinear dynamics with variable degrees/orders of stiffness. Here

Table 13 Comparison of the solution $Z_1(\xi)$ obtained by TWCM at different values of M and k , for example 4

ξ	NDSolve Solution	Taylor wavelet	AE of Haar wavelet with NDSolve	AE of FWCM with ND Solve		
				k = 1, M = 6,	k = 2, M = 6	k = 1, M = 8
0	0.00000000000000	0.00000000000000	0	0	0	0
0.1	-0.0109677919339	-0.0115093439503	6.77×10^{-2}	5.41×10^{-4}	7.78×10^{-4}	3.25×10^{-4}
0.2	-0.0119657514304	-0.0125120513519	6.57×10^{-2}	5.46×10^{-4}	6.98×10^{-5}	6.52×10^{-5}
0.3	-0.0129637088894	-0.0126880379649	6.37×10^{-2}	2.75×10^{-4}	3.39×10^{-5}	1.14×10^{-5}
0.4	-0.0139616652174	-0.0138836433091	6.16×10^{-2}	7.80×10^{-5}	5.08×10^{-5}	2.36×10^{-5}
0.5	-0.0149596194450	-0.0151704142859	5.96×10^{-2}	2.10×10^{-4}	5.25×10^{-5}	2.25×10^{-5}
0.6	-0.0159575715594	-0.0158885435374	5.75×10^{-2}	6.90×10^{-5}	4.86×10^{-5}	2.78×10^{-5}
0.7	-0.0169555215531	-0.0166749625419	1.51×10^{-1}	2.80×10^{-4}	2.86×10^{-5}	2.86×10^{-5}
0.8	-0.0179534694179	-0.0184760894456	1.53×10^{-2}	5.22×10^{-4}	7.98×10^{-5}	7.52×10^{-5}
0.9	-0.0189514151454	-0.0195452316318	5.14×10^{-2}	5.93×10^{-4}	7.80×10^{-4}	2.66×10^{-4}
1.0	-0.0199493587299	-0.0104246430262	4.93×10^{-2}	9.52×10^{-3}	9.33×10^{-3}	4.25×10^{-3}

Table 14 Comparison of the solution $Z_2(\xi)$ obtained by TWCM at diverse values of M and k , for example, 4

ξ	NDSolve solution	Taylor wavelet	AE of Haar wavelet with NDSolve	AE of FWCM with ND Solve			
				k = 1, M = 6	k = 2, M = 6	k = 1, M = 8	k = 2, M = 8
0	0.000000000000	0.000000000000	0	0	0	0	0
0.1	0.000987972928	0.0009873546106	8.79×10^{-3}	6.18×10^{-7}	5.82×10^{-7}	8.54×10^{-7}	7.78×10^{-7}
0.2	0.001985952785	0.0019853363386	8.59×10^{-3}	6.16×10^{-7}	1.23×10^{-7}	6.52×10^{-7}	6.98×10^{-7}
0.3	0.002983930647	0.0029841468735	8.39×10^{-3}	2.16×10^{-7}	7.85×10^{-7}	1.14×10^{-7}	3.39×10^{-7}
0.4	0.003981907422	0.0039819219931	8.19×10^{-4}	1.45×10^{-8}	3.26×10^{-7}	2.36×10^{-7}	5.08×10^{-7}
0.5	0.004979882134	0.0049796046590	7.98×10^{-3}	2.77×10^{-7}	2.77×10^{-7}	2.25×10^{-7}	5.25×10^{-7}
0.6	0.005977854776	0.0059778619530	7.78×10^{-4}	7.17×10^{-9}	5.23×10^{-8}	2.78×10^{-8}	4.86×10^{-8}
0.7	0.006975825338	0.0069760458570	7.58×10^{-3}	2.20×10^{-7}	2.31×10^{-7}	2.86×10^{-7}	2.86×10^{-7}
0.8	0.007973793813	0.0079731978751	7.37×10^{-3}	5.95×10^{-7}	1.95×10^{-8}	7.52×10^{-7}	7.98×10^{-7}
0.9	0.008971760192	0.0089710974988	7.17×10^{-3}	6.62×10^{-7}	3.62×10^{-7}	2.66×10^{-7}	7.80×10^{-7}
1.0	0.009969724470	0.0099793545140	3.02×10^{-3}	9.63×10^{-6}	6.63×10^{-6}	4.25×10^{-6}	9.33×10^{-6}

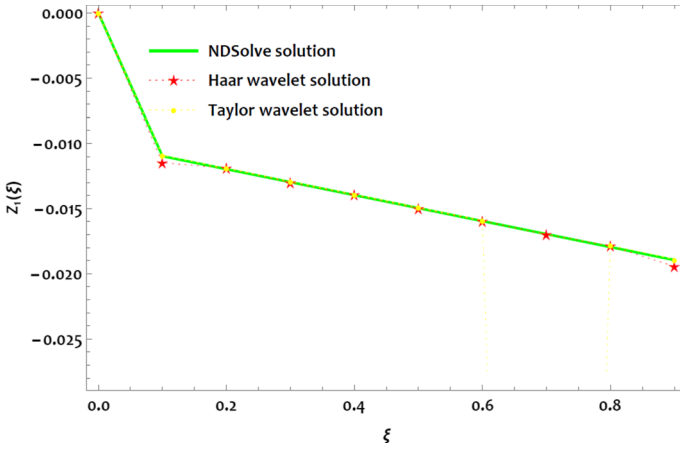


Fig. 13 Plot of the solution $Z_1(\xi)$ of example 4

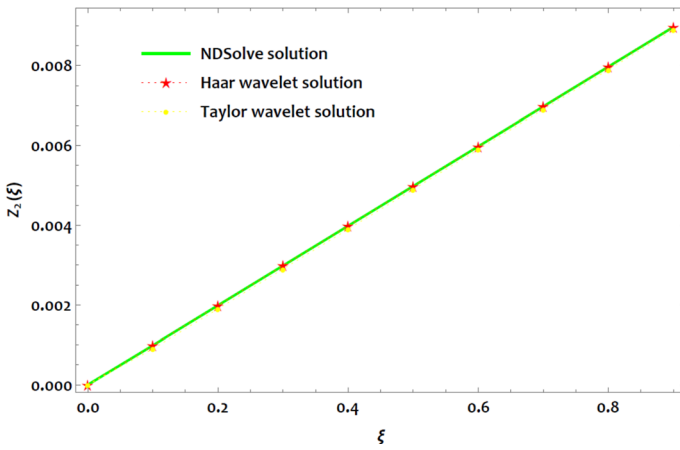


Fig. 14 Plot of the solution $Z_2(\xi)$ of example 4

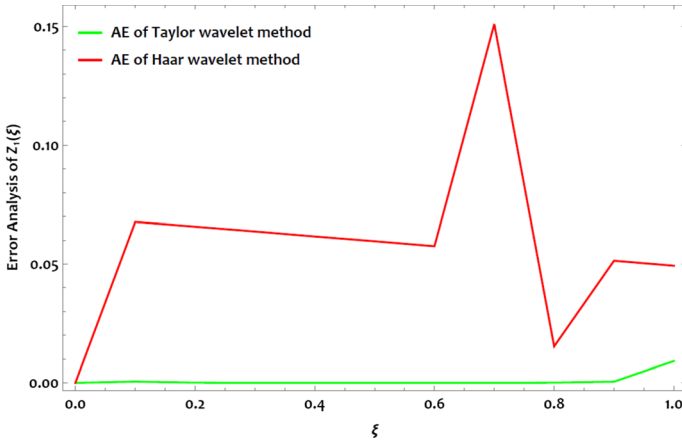


Fig. 15 Comparison of AE of the solution $Z_1(\xi)$ with different techniques, for example, 4

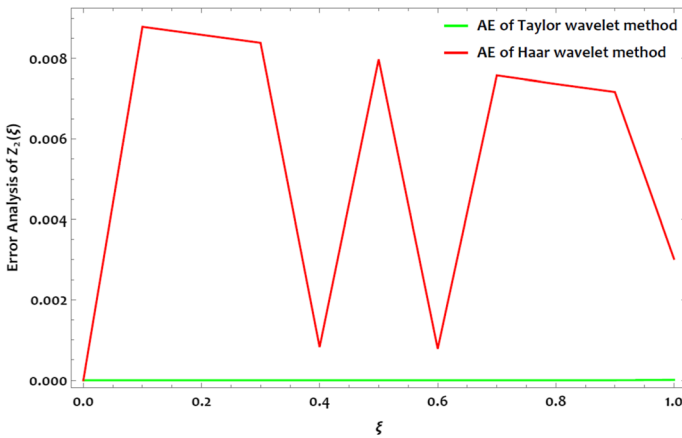


Fig. 16 Comparison of AE of the solution $Z_2(\xi)$ with different techniques, for example, 4

we have produced the Taylor wavelets' functional matrix of integration (FMI). The TWCM is implemented to attain the numerical approximation of the stiff chemical problems. The proposed method provides accurate solutions for stiff problems, whereas most numerical methods fail to give numerical solutions for stiff chemical problems. To enhance the developed method's stability and efficiency, familiar, complicated stiff systems are considered for illustration. Numerical values and absolute error of the technique in the tables and graphs strongly suggest that the proposed method is perfectly suitable to obtain the numerical solution of the stiff chemical systems. Also, tables and graphs reveal that the TWCM converges rapidly compared to other existing techniques, such as the

Haar wavelet method (HWM), Chebyshev polynomials (CMCP), Fibonacci wavelet collocation method (FWCM), and ND Solver in the literature. The method is simple and takes less computational time.

Author contributions KS proposed the main idea of this paper. KS and MG prepared the manuscript and performed all the steps of the proofs in this research. Both authors contributed equally and significantly to writing this paper. Both authors read and approved the final manuscript.

Funding The author states that no funding is involved.

Data availability and materials The data supporting this study's findings are available within the article.

Declarations

Competing interests The authors declare no competing interests.

References

1. L.F. Shampine, S. Thompson, Stiff systems. *Scholarpedia* **2**(3), 2855 (2007)
2. J. Carroll, A matricial exponentially fitted scheme for the numerical solution of stiff initial-value problems. *Comput. Math. Appl.* **26**(4), 57–64 (1993)
3. G. Hojjati, M.R. Ardabili, S.M. Hosseini, A-EBDF: an adaptive method for the numerical solution of stiff systems of ODEs. *Math. Comput. Simul.* **66**(1), 33–41 (2004)
4. J.R. Cash, the integration of stiff initial value problems in ODEs using modified extended backward differentiation formulae. *Comput. Math. Appl.* **9**(5), 645–657 (1983)
5. S.M. Hosseini, G. Hojjati, Matrix-free MEBDF method for the solution of stiff systems of ODEs. *Math. Comput. Model.* **29**(4), 67–77 (1999)
6. C.H. Hsiao, Haar wavelet approach to linear stiff systems. *Math. Comput. Simul.* **64**(5), 561–567 (2004)
7. N.M. Bujurke, C.S. Salimath, S.C. Shiralashetti, Numerical solution of stiff systems from nonlinear dynamics using single-term Haar wavelet series. *Nonlinear Dyn.* **51**, 595–605 (2008)
8. M.T. Darvishi, F. Khani, A.A. Soliman, The numerical simulation for stiff systems of ordinary differential equations. *Comput. Math. Appl.* **54**(7–8), 1055–1063 (2007)
9. G. Bader, P. Deuffhard, A semi-implicit mid-point rule for stiff systems of ordinary differential equations. *Numer. Math.* **41**(3), 373–398 (1983)
10. A. Prothero, A. Robinson, On the stability and accuracy of one-step methods for solving stiff systems of ordinary differential equations. *Math. Comput.* **28**(125), 145–162 (1974)
11. S. Dhawan, J.A.T. Machado, D.W. Brzeziński, M.S. Osman, A Chebyshev wavelet collocation method for some types of differential problems. *Symmetry*. **13**(4), 536 (2021)
12. M. Faheem, A. Raza, A. Khan, Collocation methods based on Gegenbauer and Bernoulli wavelets for solving neutral delay differential equations. *Math. Comput. Simul.* **180**, 72–92 (2021)
13. S. Kumbinarasaiah, K.R. Raghunatha, the applications of the Hermite wavelet method to nonlinear differential equations arising in heat transfer. *Int. J. Thermofluids*. **9**, 100066 (2021)
14. S. Kumbinarasaiah, M. Mulimani, A study on the non-linear Murray equation through the Bernoulli wavelet approach. *Int. J. Appl. Comput. Math.* **9**(3), 40 (2023)
15. S. Kumbinarasaiah, R.A. Mundewadi, Numerical solution of fractional-order integro-differential equations using the Laguerre wavelet method. *J. Inf. Optim. Sci.* **43**(4), 643–662 (2022)
16. T. Abdeljawad, R. Amin, K. Shah, Q. Al-Mdallal, F. Jarad, Efficient sustainable algorithm for numerical solutions of systems of fractional order differential equations by Haar wavelet collocation method. *Alex. Eng. J.* **59**(4), 2391–2400 (2020)
17. S. Erman, A. Demir, E. Ozbilge, solving inverse nonlinear fractional differential equations by generalized Chelyshkov wavelets. *Alex. Eng. J.* **66**, 947–956 (2023)
18. S. Kumbinarasaiah, M. Mulimani, The Fibonacci wavelets approach for the fractional Rosenau-Hyman equations. *Results Control Optim.* **11**, 100221 (2023)

19. X. Li, Numerical solution of fractional differential equations using cubic B-spline wavelet collocation method. *Commun. Nonlinear Sci. Numer. Simul.* **17**(10), 3934–3946 (2012)
20. L.I. Yuanlu, solving a nonlinear fractional differential equation using Chebyshev wavelets. *Commun. Nonlinear Sci. Numer. Simul.* **15**(9), 2284–2292 (2010)
21. A. Isah, C. Phang, Genocchi wavelet-like operational matrix and its application for solving nonlinear fractional differential equations. *Open Physics.* **14**(1), 463–472 (2016)
22. E. Keshavarz, Y. Ordokhani, M. Razzaghi, Bernoulli wavelet operational matrix of fractional order integration and its applications in solving the fractional order differential equations. *Appl. Math. Model.* **38**(24), 6038–6051 (2014)
23. S. Kumbinarasaiah, G. Manohara, G. Hariharan, Bernoulli wavelets functional matrix technique for a system of nonlinear singular Lane Emden equations. *Math. Comput. Simul.* **204**, 133–165 (2022)
24. S. Kumbinarasaiah, G. Manohara, Modified Bernoulli wavelets functional matrix approach for the HIV infection of CD4+ T cells model. *Results Control Optim.* **10**, 100197 (2023)
25. F. Mohammadi, C. Cattani, A generalized fractional-order Legendre wavelet Tau method for solving fractional differential equations. *J. Comput. Appl. Math.* **339**, 306–316 (2018)
26. S. Kumbinarasaiah, Hermite wavelets approach for the multi-term fractional differential equations. *J. Interdiscip. Math.* **24**(5), 1241–1262 (2021)
27. S. Kumbinarasaiah, W. Adel, Hermite wavelet method for solving nonlinear Rosenau-Hyman equation. *Partial Differ. Equ. Appl. Math.* **4**, 100062 (2021)
28. M. Rehman, U. Saeed, Gegenbauer wavelets operational matrix method for fractional differential equations. *J. Korean Math. Soc.* **52**(5), 1069–1096 (2015)
29. E. Keshavarz, Y. Ordokhani, M. Razzaghi, The Taylor wavelets method for solving the initial and boundary value problems of Bratu-type equations. *Appl. Numer. Math.* **128**, 205–216 (2018)
30. P.T. Toan, T.N. Vo, M. Razzaghi, Taylor wavelet method for fractional delay differential equations. *Eng. Comput.* **37**, 231–240 (2021)
31. T.N. Vo, M. Razzaghi, P.T. Toan, Fractional-order generalized Taylor wavelet method for systems of nonlinear fractional differential equations with application to human respiratory syncytial virus infection. *Soft. Comput.* **26**, 165–173 (2022)
32. S.C. Shiralashetti, S.I. Hanaji, Taylor wavelet collocation method for Benjamin–Bona–Mahony partial differential equations. *Results Appl. Math.* **9**, 100139 (2021)
33. I. Dağ, A. Canıvar, A. Şahin, Taylor-Galerkin and Taylor-collocation methods for the numerical solutions of Burgers' equation using B-splines. *Commun. Nonlinear Sci. Numer. Simul.* **16**(7), 2696–2708 (2011)
34. F. Li, H.M. Baskonus, S. Kumbinarasaiah, G. Manohara, W. Gao, E. Ilhan, An efficient numerical scheme for biological models in the frame of Bernoulli wavelets. *Comput. Model. Eng. Sci.* **137**, 3 (2023)
35. S. Gümgüm, Taylor wavelet solution of linear and nonlinear Lane-Emden equations. *Appl. Numer. Math.* **158**, 44–53 (2022)
36. G. Manohara, S. Kumbinarasaiah, Fibonacci wavelets operational matrix approach for solving chemistry problems. *J. Umm Al-Qura Univ. Appl. Sci.* (2023). <https://doi.org/10.1007/s43994-023-00046-5>
37. G. Hariharan, K. Kannan, Review of wavelet methods for the solution of reaction–diffusion problems in science and engineering. *Appl. Math. Model.* **38**(3), 799–813 (2014)
38. G. Hariharan, R. Rajaraman, A new coupled wavelet-based method applied to the nonlinear reaction–diffusion equation arising in mathematical chemistry. *J. Math. Chem.* **51**, 2386–2400 (2003)
39. G. Hariharan, K. Kannan, K.R. Sharma, Haar wavelet method for solving Fisher's equation. *Appl. Math. Comput.* **211**(2), 284–292 (2009)
40. G. Hariharan, G.K. Kannan, Haar wavelet method for solving some nonlinear parabolic equations. *J. Math. Chem.* **48**, 1044–1061 (2010)
41. S. Kumbinarasaiah, M. Mulimani, Fibonacci wavelets-based numerical method for solving fractional order $(1 + 1)$ -dimensional dispersive partial differential equation. *Int. J. Dyn. Control* **11**, 2232–2255 (2023)
42. M.M. Khalsaraci, A. Shokri, M. Molayi, The new class of multistep multiderivative hybrid methods for the numerical solution of chemical stiff systems of first order IVPs. *J. Math. Chem.* **58**, 1987–2012 (2020)
43. Y. Öztürk, Numerical solution of systems of differential equations using operational matrix method with Chebyshev polynomials. *J. Taibah Univ. Sci.* **12**(2), 155–162 (2018)

Publisher's Note Springer Nature remains neutral with regard to jurisdictional claims in published maps and institutional affiliations.

Springer Nature or its licensor (e.g. a society or other partner) holds exclusive rights to this article under a publishing agreement with the author(s) or other rightsholder(s); author self-archiving of the accepted manuscript version of this article is solely governed by the terms of such publishing agreement and applicable law.